Seasonal dynamics of atmospheric and river inputs of black carbon, and impacts on biogeochemical cycles in Halong Bay, Vietnam

Xavier Mari, Thuoc Chu Van, Benjamin Guinot, Justine Brune, Jean-Pierre Lefebvre, Patrick Raimbault, Thorsten Dittmar, Jutta Niggemann

ELEMENTA
Science of the Anthropocene

Mari, X, et al. 2017 Seasonal dynamics of atmospheric and river inputs of black carbon, and impacts on biogeochemical cycles in Halong Bay, Vietnam. *Elem Sci Anth,* 5: 75. DOI: https://doi.org/10.1525/elementa.255

RESEARCH ARTICLE

Seasonal dynamics of atmospheric and river inputs of black carbon, and impacts on biogeochemical cycles in Halong Bay, Vietnam

Xavier Mari[*,†], Thuoc Chu Van[‡], Benjamin Guinot[§], Justine Brune[‖], Jean-Pierre Lefebvre[¶,**], Patrick Raimbault[*], Thorsten Dittmar[††] and Jutta Niggemann[††]

Emissions of black carbon (BC), a product of incomplete combustion of fossil fuels, biofuels and biomass, are high in the Asia-Pacific region, yet input pathways and rates to the ocean are not well constrained. Atmospheric and riverine inputs of BC in Halong Bay (Vietnam), a hotspot of atmospheric BC, were studied at monthly intervals during one year. Climate in Halong Bay is governed by the monsoon regime, characterized by a northeast winter monsoon (dry season) and southeast summer monsoon (wet season). During the dry season, atmospheric BC concentrations averaged twice those observed during the wet season. In the sea surface microlayer (SML) and underlying water (ULW), concentrations of particulate BC (PBC) averaged 539 and 11 µmol C L^{-1}, respectively. Dissolved BC (DBC) concentrations averaged 2.6 µmol C L^{-1} in both the SML and ULW. Seasonal variations indicated that PBC concentration in the SML was controlled by atmospheric deposition during the dry season, while riverine inputs controlled both PBC and DBC concentrations in ULW during the wet season. Spatiotemporal variations of PBC and DBC during the wet season suggest that river runoff was efficient in transporting PBC that had accumulated on land during the dry season, and in mobilizing and transporting DBC to the ocean. The annual river flux of PBC was about 3.8 times higher than that of DBC. The monsoon regime controls BC input to Halong Bay by favoring dry deposition of BC originating from the north during the dry season, and wet deposition and river runoff during the wet season. High PBC concentrations seem to enhance the transfer of organic carbon from dissolved to particulate phase by adsorbing dissolved organic carbon and stimulating aggregation. Such processes may impact the availability and biogeochemical cycling of other dissolved substances, including nutrients, for the coastal marine ecosystem.

Keywords: Black carbon; Atmospheric deposition; River input; Sea surface microlayer; Dissolved organic carbon; Particulate organic carbon

1. Introduction

Black carbon (BC) is the product of incomplete combustion of fossil fuels, biofuels and biomass, and is a major component of soot which encompasses both black and organic carbon (OC). BC and CO_2 are "carbon cousins", both produced by burning, regardless of the fuel source. Global estimates indicate that 2 to 29 Tg BC are emitted per year (Bond et al., 2013). In the atmosphere, BC defines a continuum from freshly emitted single nanospheres (aerodynamic diameter < 50 nm) to aged

* Aix Marseille Université, Université de Toulon, CNRS, IRD, Mediterranean Institute of Oceanography (MIO), 13288 Marseille, FR

† Sorbonne Universités, UPMC, Université Paris 06, UMR 7093, CNRS, Laboratoire d'Océanographie de Villefranche (LOV), 181 Chemin du Lazaret, 06230 Villefranche-sur-Mer, FR

‡ Institute of Marine Environment and Resources (IMER), Vietnam Academy of Science and Technology (VAST), 246 Da Nang Street, Haiphong, VN

§ Laboratoire d'Aérologie (LA), Université de Toulouse, CNRS, UPS, 14 Avenue Edouard-Belin, 31400 Toulouse, FR

‖ UMR 5119 ECOSYM, Université Montpellier II, Case 093, Place Bataillon, 34095 Montpellier, FR

¶ UMR 5566 LEGOS, Université de Toulouse, 14 avenue Édouard Belin, 31400 Toulouse, FR

** Center for Environmental Fluid Dynamics, University of Science, Vietnam National University, 334 Nguyen Trai, Hanoi, VN

†† Research Group for Marine Geochemistry (ICBM-MPI Bridging Group), University of Oldenburg, Institute for Chemistry and Biology of the Marine Environment, 26129 Oldenburg, DE

Corresponding author: Xavier Mari (xavier.mari@ird.fr)

grape-like aggregates of tens of micrometers (Marrero et al., 2007; Long et al., 2013), the chemical nature of which ranges from pure to highly functionalized carbon chains, respectively (Goldberg, 1985). In the atmosphere, BC is associated with other aerosols such as sulfates, nitrates, metals and organic acids (Guazzotti et al., 2001). All together, these aerosols form what are called atmospheric brown clouds, which are known to concentrate in specific regional hot-spots, the most important being located in Asia, in accordance with hot-spots of BC emissions. These hot-spots of increased atmospheric BC concentration give rise to widespread atmospheric plumes allowing long range transport and deposition over adjacent oceans (Hadley et al., 2007; Ramanathan et al., 2007; Ramanathan and Carmichael, 2008; Lin et al., 2014).

The atmospheric lifetime of BC is short and ranges from a few days in rainy climates up to one month in dry regions (Ogren and Charlson, 1983) providing enough time for BC to reach even the most remote oceanic sites. Black carbon leaves the atmosphere via dry or wet deposition on land and on the ocean. On a global scale, deposition on the ocean is estimated to range from about 7 Tg C yr^{-1} (Suman et al., 1997) to 12 Tg C yr^{-1} (Jurado et al., 2008). Although BC can travel over long distances and cross oceans (Hadley et al., 2007), its short lifetime in the atmosphere implies that deposition on the ocean occurs preferentially in the vicinity of the source of emission; i.e., in the coastal zone and along shipping routes (Corbett et al., 2007; Johansson et al., 2017).

In addition to direct atmospheric deposition on the surface of the ocean, BC also reaches the marine system via river runoff. While atmospheric BC is defined only as particulate, with BC particles ranging in size from about 50 nm to tens of micrometers, BC in a water sample can be size-separated by filtration (common size cut-off of 0.7 μm) into the fraction retained on the filter (particulate) and that passing through the filter (dissolved). As a result, BC concentrations in marine systems are reported for both particulate and dissolved phases. About 10% of the riverine pool of dissolved organic carbon (DOC) is dissolved BC (DBC), which at the global scale brings this input pathway to the ocean to about 26 Tg dissolved BC yr^{-1} (Jaffé et al., 2013). A recent study conducted in the two largest rivers in China found that the concentration of particulate BC (PBC) was 4.1 to 6.7 times higher than that of DBC (Wang et al., 2016). As a result, riverine input of BC, both in dissolved and particulate phase, appears to be a major source of BC in the coastal zone, and particularly in highly BC-impacted regions.

Therefore, while aeolian transport is the most important source of open-ocean BC (Suman et al., 1997; Masiello and Druffel, 1998), riverine and surface runoff may be the dominant source of BC in the coastal zone (Mitra et al., 2002; Mannino and Harvey, 2004). In the coastal zone, the aeolian and riverine pathways of BC input are subject to different seasonal forcing linked to variations of BC concentration in the atmosphere and of the precipitation regime.

North Vietnam is governed by the monsoon regime, characterized by the alternation of a dry winter season coinciding with high atmospheric BC concentrations, and of a wet summer season coinciding with low atmospheric BC concentrations (Hien et al., 2002, 2004; Gatari et al., 2006). Therefore, the input of BC to the coastal zone in this region is expected to be dominated by dry deposition during the winter monsoon, and dominated by wet deposition and riverine runoff during the summer monsoon. Because in the Asia-Pacific region, the emission of BC to the atmosphere is expected to increase in the coming decades (OECD, 2016), in particular due to the rising use of coal-fired power plants (Koplitz et al., 2017), it is relevant to define and constrain the pathways for BC into the ocean, as well as its impact on marine ecosystems.

Here, we present comprehensive data on the distribution and seasonal variation of dissolved and particulate BC and related biogeochemical parameters in a highly BC-impacted coastal system (Halong Bay, North Vietnam). The aims of this study were (1) to evaluate the two main gateways for BC input to the marine system (i.e., the sea surface microlayer, which is the pathway for atmospheric deposition, and the main estuary of the bay, which is the pathway for riverine input of BC) and (2) to critically assess the impact of high BC inputs in Halong Bay surface waters.

2. Methods

2.1. Study site

This study has been conducted in Halong Bay, North Vietnam (**Figure 1**). Halong Bay, which has been inscribed in 2000 on the UNESCO's World Heritage List, expands to about 1,600 km^2, includes some 2,000 islands and islets, and has a maximum depth of less than 15 m. Halong Bay is bordered in the south and southeast by the Gulf of Tonkin, in the north by the Quang Ninh province and in the west and southwest by Cat Ba Island. The climate in this area is governed by the monsoon regime, characterized by a northeast winter monsoon from October to May (dry season), and a southeast summer monsoon from May to October (wet season). This site is located in one of the hotspots of atmospheric BC concentration (Ramanathan et al., 2007; Ramanathan and Carmichael, 2008), with typical concentrations of about 3 μg BC m^{-3} (Hien et al., 2004; Gatari et al., 2006) and highest concentrations during the winter monsoon (Hien et al., 2002). A study of 48-h back trajectories using Halong Bay as the endpoint and over the period October 2012–November 2013, has shown that air masses originate primarily from the northeast and from the south, respectively, during the dry and wet seasons (B Guinot, personal communication).

2.2. Sampling

Seawater samples were collected along a transect of four stations (A, B, C and D; **Figure 1**), at about monthly intervals (14 sampling occasions), during a complete annual cycle from 15 October 2012 to 24 October 2013, using a 15-m coastal vessel. CTD profiles were acquired with a SBE19+ probe (Sea-Bird Electronics). Station A is located at the mouth of Cua Luc Bay, a shallow "lagoon-type" estuary of less than 20 km^2 (with an estimated volume of 34×10^6 m^3) at the confluence of three main

tributaries, the rivers Dien Vong, Man and Troi. These rivers have a catchment basin of 610 km^2 (Son, 2007). The discharge of the rivers ranges from several cubic meters per second during the dry season to up to 1,500 m^3 s^{-1} during the wet season (Ho et al., 2013).

The water depths at stations A, B, C and D were 11, 4, 13 and 9 m, respectively. Seawater samples were collected at 1.5-m depth (hereafter called underlying water; ULW) using a 5-L Niskin bottle. Sea surface microlayer (SML) samples were collected from the bow of the boat (1 m above sea level) using a glass plate sampler by vertically dipping, slowly withdrawing, and collecting water adhering to the glass plate directly into Nalgene bottles (**Figure 2**). Because each dipping of the SML sampler allows collecting only about 8 mL of SML, the glass plate was dipped repeatedly through the SML in order to collect

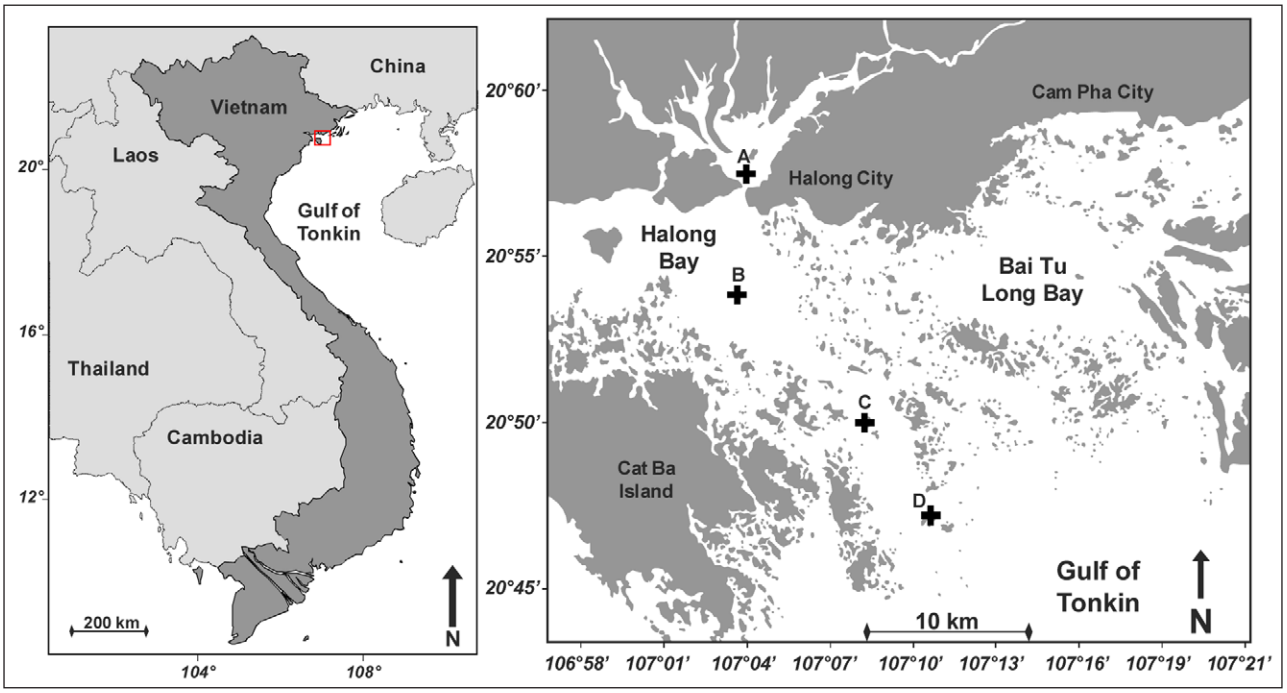

Figure 1: Maps of the sampling location. Maps showing the location of Halong Bay in North Vietnam (left panel; red square), and the position of the four sampling stations (right panel; black crosses denote stations A, B, C and D). Station A is located in Cua Luc Bay. DOI: https://doi.org/10.1525/elementa.255.f1

Figure 2: Black carbon slick and SML sampling. Example of a black slick observed in Halong Bay during the dry season (left), and sea surface microlayer (SML) sampling (right) using the glass plate technique within such highly BC-impacted slicks. Note the color of the SML sample; although visually resembling an oil slick in situ, analyses confirmed these black slicks were due to BC. DOI: https://doi.org/10.1525/elementa.255.f2

enough seawater from the SML (about 1 L) for conducting the different analyses.

After sampling, seawater samples were immediately processed onboard for later analyses of chlorophyll *a* (Chl *a*), dissolved organic carbon (DOC), dissolved BC (DBC), dissolved organic nitrogen and phosphorus (DON and DOP), inorganic nutrients (NO_2^-, NO_3^-, NH_4^+, PO_4^{3-}), particulate organic carbon and nitrogen (POC and PON), and particulate BC (PBC). Enrichment factors (EF), calculated for each parameter as concentration in the SML divided by respective concentration in ULW, were used to determine the enrichment pathways, i.e., atmospheric deposition versus riverine inputs.

2.3. Seasonal concentration of atmospheric BC and weather conditions

Atmospheric BC concentrations were monitored every two weeks for 24 h from October 2012 to October 2013, from PM_{10} aerosol samples collected onto Staplex Type TFAQ810 Quartz Fiber Filters (20 × 25 cm) using a Staplex PM_{10} High Volume Air sampler installed on the roof of the IMER building, in Haiphong City, at approximately 30 km from Halong Bay. The average (± standard deviation, SD) air volume filtered through the Staplex Quartz Fiber Filters during the 24-h sampling, calculated from the recorded instantaneous air flow rate, was 1147 ± 126 m^3 $filter^{-1}$. After sampling, each quartz filter was stored individually in a sealed plastic bag and frozen until analysis. Concentrations of atmospheric BC, OC, total nitrogen (TN) and total phosphorus (TP) were measured from circular patches of 25-mm diameter, cut out of the Staplex Quartz Fiber Filters using a Boehm® hollow punch, following the analytical protocols described below.

Atmospheric BC concentrations were also monitored in real-time during each field sampling, using a field micro-aethalometer (MicroAeth® Model AE51; AethLabs, San Francisco, CA, USA) installed on the roof of the boat at about 5 m above sea level. The sampling/logging time interval was set to 1 min. The aethalometer provides a real-time optical readout of the concentration of atmospheric BC particles. As indicated by its name, black carbon is defined by blackness, an optical measurement. Its light-adsorbing property is used by the aethalometer that collects the sample on a quartz fiber filter tape to perform a continuous optical analysis.

Meteorological data (wind speed and direction, and rainfall) were recorded continuously during the complete annual cycle from a weather station (Vantage Pro2; Davis Instruments) installed in Haiphong City, next to the PM_{10} sampler.

2.4. Pigments

Chlorophyll *a* (Chl *a*) was determined fluorometrically on methanol-extracted samples from 100-mL subsamples filtered onto 25-mm Whatman GF/F filters using the method described by Holm-Hansen et al. (1965). Immediately after filtration onboard, filters were placed in 2-mL plastic tubes and stored in liquid nitrogen until analysis in the laboratory.

2.5. Inorganic nutrients, and dissolved organic nitrogen and phosphorus determination

Analyses of nitrate (NO_3^-), nitrite (NO_2^-), ammonium (NH_4^+), phosphate (PO_4^{3-}), DON and DOP were conducted on duplicate 30-mL sub-samples filtered through 47-mm pre-combusted (450°C overnight) Whatman GF/F filters and collected in acid washed 30-mL Nalgene flasks (soaked in 10% HCl). Samples were filtered onboard and the flasks were immediately placed in a cool box filled with ice (< 4°C) prior to pasteurization (80 ± 3°C for 6 h; Daniel et al., 2005) in the laboratory. After pasteurization, the flasks were stored in the dark until analysis.

Nutrient concentrations were measured with an AutoAnalyseur III Seal Bran Luebbe (Mequon, USA) according to Aminot and Kerouel (2007). To achieve reproducible nutrient measurements, standards were used and compared to commercially available products (OSIL). The detection limits of NO_3^-, NO_2^- and PO_4^{3-} were 0.05, 0.05 and 0.02 μmol L^{-1}, respectively.

Determination of total (i.e., sum of organic and inorganic) nitrogen (TN) and phosphorus (TP) was carried out simultaneously on the same samples using the wet-oxidation procedure described in Raimbault et al. (1999), where persulfate was used to digest the organic matter, and the inorganic end-products determined by colorimetry. Dissolved organic nitrogen (DON) and dissolved organic phosphorus (DOP) were calculated as TN and TP minus dissolved inorganic nitrogen (DIN; nitrate + nitrite + ammonium) or phosphate measured in the same samples. The analytical accuracy, determined on replicates of reference samples, was close to 0.5 and 0.05 μmol L^{-1} for DON and DOP, respectively.

2.6. Dissolved organic carbon determination

In order to distinguish between non-pyrogenic dissolved organic carbon (DOC) and dissolved BC (DBC) within total dissolved organic carbon (T-DOC), we used a combination of analytical procedures. The concentrations of T-DOC were measured using a Shimadzu TOC VCPH, and the concentrations of DBC were measured using an ultrahigh performance liquid chromatography system on dissolved organic matter (DOM) extracts obtained by solid-phase extraction. Non-pyrogenic DOC (i.e., thermally unaltered DOC) is defined as the fraction of T-DOC that is not targeted by the benzenepolycarboxylic acids method used to measure DBC concentration (see below). Non-pyrogenic DOC was obtained by subtracting DBC from T-DOC.

Analyses of T-DOC were performed on 20-mL subsamples immediately filtered through 47 mm pre-combusted Whatman GF/F filters and collected in pre-combusted (450°C, overnight) 24-mL glass tubes, preserved with 24 μL of 85% phosphoric acid (H_3PO_4). Samples were stored in the dark until analysis. T-DOC concentration was measured on a Shimadzu TOC VCPH analyzer with potassium phthalate calibration standards over the measurement range of 0–400 μmol C L^{-1}.

Certified reference materials (Hansell Laboratory, University of Miami, Florida) were used as external standards to determine the machine blank. Both the low carbon

water (LCW, ~1 μmol C L^{-1}) and the deep seawater (DSW, ~45.5 μmol C L^{-1}) standards were used at the beginning of each sample run (i.e., every 10 samples). Milli-Q blanks were regularly injected as "sample blanks" during the analysis sequence to ensure that no sample carryover was observed. The machine blank, calculated for each run of 10 samples, as $[(LCW_{measured} - 1) + (DSW_{measured} - 45.5)]/2$, averaged –8.3 ± 2.6 μmol C L^{-1}. The reported T-DOC values were blank-corrected by subtracting the machine blank obtained at the beginning of each sample run.

Samples for DBC analyses were collected and prepared according to the solid-phase extraction (SPE) method (Dittmar et al., 2008). This method allows concentrating DOM molecules (including DBC) in salt-free methanol extracts. Briefly, for each sampling occasion, 500 mL of SML and 500 mL of ULW samples were filtered through pre-combusted (450°C overnight) 47-mm diameter GF/F filters, directly into acid-washed polycarbonate bottles and immediately acidified with hydrochloric acid 37% to reach a pH of 2. The bottles were stored in a cool box filled with ice (< 4°C) until SPE procedure in the laboratory. Solid phase extractable DOM is referred to as SPE-DOM in the following. Cartridges filled with Varian Bond Elut sorbents (PPL) were used to concentrate DOM. PPL sorbent consists of a styrene divinyl copolymer and is made for the retention of highly polar to non-polar substances from large volumes of water. The cartridges were rinsed with methanol (HPLC grade) immediately before use. The filtered and acidified samples were gravity-processed through the cartridges at a flow rate of < 15 mL min^{-1}. Immediately after extraction, remaining salts were washed off the cartridges with 40 mL of pH 2 ultrapure water (LC/MS Reagent, JT Baker® 9831-03). The cartridges were dried under a N_2 stream, before elution of the SPE-DOM with 8 mL of methanol. The eluates were stored in acid-rinsed 8-mL vials at –18°C until analysis.

DBC was analyzed as benzenepolycarboxylic acids (BPCAs) after nitric acid oxidation following the method of Dittmar (2008). Aliquots of 1 mL extract, corresponding to 2–8 μmol of SPE-DOC, were transferred to combusted (450°C, 4 h) glass ampoules and dried overnight at 50°C. Dry extracts were dissolved in 500 μL of nitric acid (65%), ampoules were sealed and placed in a pressure bomb to be heated for 9 h at 170°C. After cooling, 450 μL of the solution were transferred to sample vials and evaporated to dryness in a vacuum centrifuge (Christ RV2-18). Samples were dissolved in 100 μl of phosphate buffer (pH 7.2) and analyzed on an ultrahigh performance liquid chromatography system (UPLC, Waters Acquity) equipped with a photodiode array absorbance detector. BPCAs were identified based on retention time and absorbance spectra (220–380 nm) and quantified using four-point calibration curves and the respective absorbance signal at 240 nm. DBC concentrations were calculated from BPCA concentrations as outlined in Dittmar (2008), with the modification detailed in Stubbins et al. (2015). Procedural blanks did not yield any detectable amounts of BPCAs.

2.7. Particulate organic carbon and nitrogen determination

In order to distinguish between non-pyrogenic particulate organic carbon (POC) and particulate BC (PBC) within total particulate organic carbon (T-POC), we used a combination of analytical procedures, as follows. Total particulate organic carbon (T-POC), particulate BC (PBC) and particulate organic nitrogen (PON) were measured from duplicate 100-mL subsamples immediately filtered onboard onto pre-combusted (450°C overnight) 25-mm Whatman GF/F filters. One subsample was used to measure T-POC; the other was used to measure PBC. The concentration of non-pyrogenic POC was calculated for each sample as the difference between PBC and T-POC concentration. After filtration, the filters were individually placed in 2-mL plastic tubes and immediately frozen in liquid nitrogen. In the laboratory, filters were dried at 60°C for 24 h and stored in sealed plastic bags until analysis.

For PBC analyses, non-pyrogenic POC (i.e., thermally unaltered POC) was removed by a chemothermal oxidation (CTO) pre-treatment of the filters at 340 ± 0.5°C for 2 h and under an oxidative gas (pure oxygen) flow to prevent charring during the treatment (Cachier et al., 1989; Kuhlbusch, 1995). According to Nguyen et al. (2004), this CTO pre-treatment in oxygen at 340°C yields similar results for soot as CTO in air at 375°C, and the remaining carbon on the filters is operationally defined as BC (Kuhlbusch, 1995; Gustafsson et al., 1997).

Prior to the determination of particulate carbon (i.e., T-POC and PBC), all of the filters were acidified with 100 μL of 0.5 N H_2SO_4 in order to remove inorganic carbon. Acidified samples were kept in a drying oven (60°C) until analyses. Particulate carbon (both T-POC and PBC) and particulate nitrogen were determined by high temperature combustion (900°C) performed on a CN Integra mass spectrometer (Raimbault et al., 2008). The same CTO protocol was used on the Staplex quartz filters for determining the concentrations of atmospheric BC and atmospheric organic carbon (OC).

3. Results

3.1. Weather conditions and characteristics of aerosols

The seasonal rainfall regime recorded from October 2012 to October 2013 only differed from the typical monsoon regime of the region by sporadic heavy rainfall events that occurred in November–December, during the early phase of the dry season (**Figure 3**). The total volume of freshwater injected into Halong Bay from the watershed of the Cua Luc Bay, calculated from the size of the watershed (610 km^2) and from annual precipitation data obtained from the weather station in Haiphong City (4332 mm), reached an annual volume of 2.64×10^9 m^3 yr^{-1}. The wind regime was dominated by weak northeasterly winds during the dry season (from October 2012 to April 2013) and by strong southeasterly winds during the wet season (from May to September 2013) (**Figure 4**).

The concentrations of both atmospheric BC and OC in PM_{10} during the dry season were on average about twice those recorded during the wet season (**Figure 5**). The

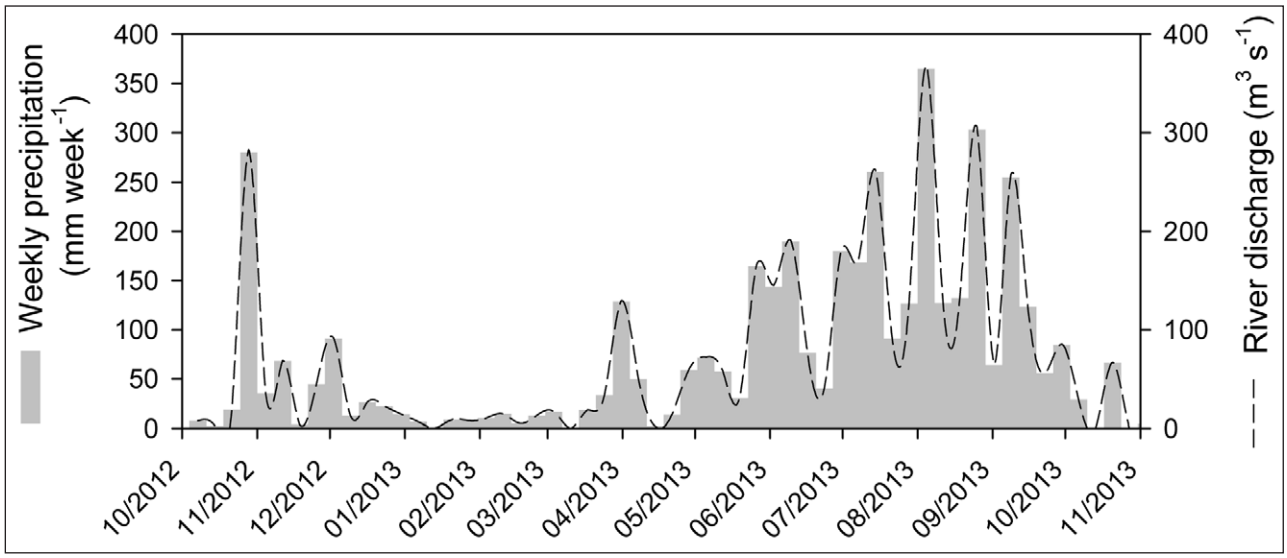

Figure 3: Seasonal variations of precipitation and freshwater discharge. Weekly variations of precipitation and freshwater discharge from the Cua Luc Bay watershed. Freshwater discharge was estimated from the size of the watershed (610 km^2) and weekly precipitation data. DOI: https://doi.org/10.1525/elementa.255.f3

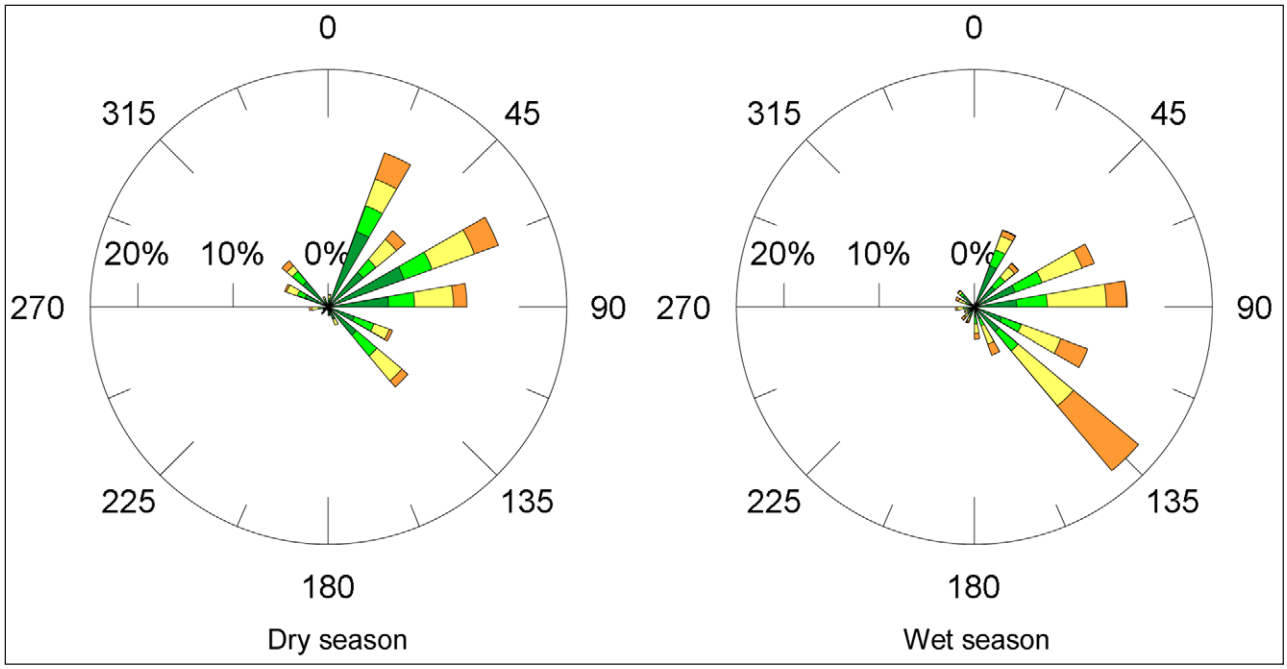

Figure 4: Seasonal wind regime. Wind regime during the dry (left panel) and wet (right panel) seasons. The wind speed bins are: (dark green) ≤ 1 m s^{-1}, (light green) > 1 to 1.5 m s^{-1}, (yellow) > 1.5 to 2.5 m s^{-1} and (orange) > 2.5 to 5 m s^{-1}. DOI: https://doi.org/10.1525/elementa.255.f4

concentrations of atmospheric BC in PM_{10} collected in Haiphong City averaged 2.60 ± 1.25 μg m^{-3} (n = 18) and 1.12 ± 0.70 μg m^{-3} (n = 9) during the dry and wet seasons, respectively, and were significantly higher during the dry season (*t*-test, $p < 0.05$). The same seasonal pattern was observed for atmospheric BC concentrations measured with the aethalometer during sampling in Halong Bay, with average concentrations significantly higher (*t*-test, $p < 0.05$) during the dry season (4.66 ± 2.86 μg m^{-3}, n = 14533) in comparison with the wet season (2.28 ± 1.44 μg m^{-3}, n = 13693).

The concentrations of atmospheric OC in PM_{10} showed the same seasonal pattern as atmospheric BC, with an average of 5.54 ± 2.56 μg m^{-3} (n = 18) and 2.62 ± 1.38 μg m^{-3} (n = 9) during the dry and wet seasons, respectively, and were significantly higher during the dry season (*t*-test, $p < 0.05$), suggesting that dry deposition of atmospheric BC on the sea surface of Halong Bay should be higher during the dry season than the wet season. A similar seasonal pattern was observed for the concentrations of total nitrogen (TN) and total phosphorus (TP) in PM_{10} (**Figure 6**), suggesting that the deposition of

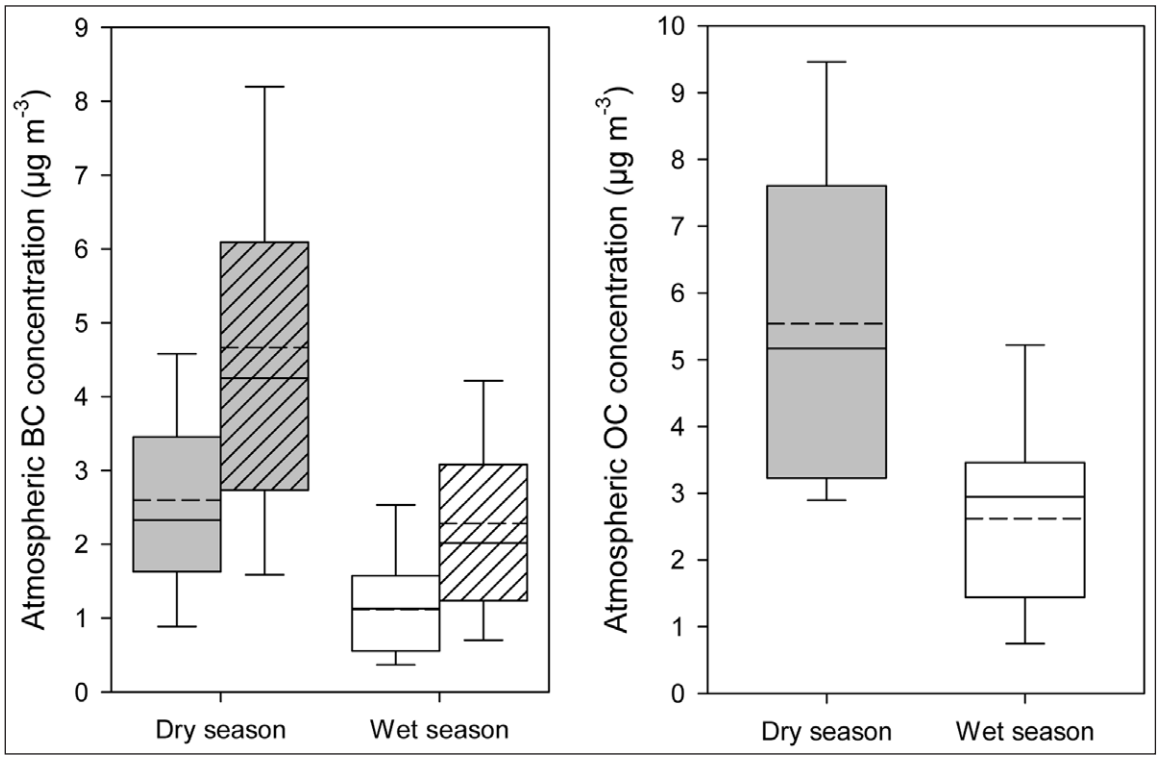

Figure 5: Concentrations of atmospheric black carbon and organic carbon. Seasonal variations of atmospheric BC (left panel) and atmospheric OC concentrations (right panel). The BC concentrations were measured both from PM_{10} collected in Haiphong City using the CTO method (plain box) and from real-time measurements in Halong Bay using the aethalometer (hatched box). Box-and-whisker plots showing median (straight line) and average (dashed line) concentrations. Note different scales for the y-axes. DOI: https://doi.org/10.1525/elementa.255.f5

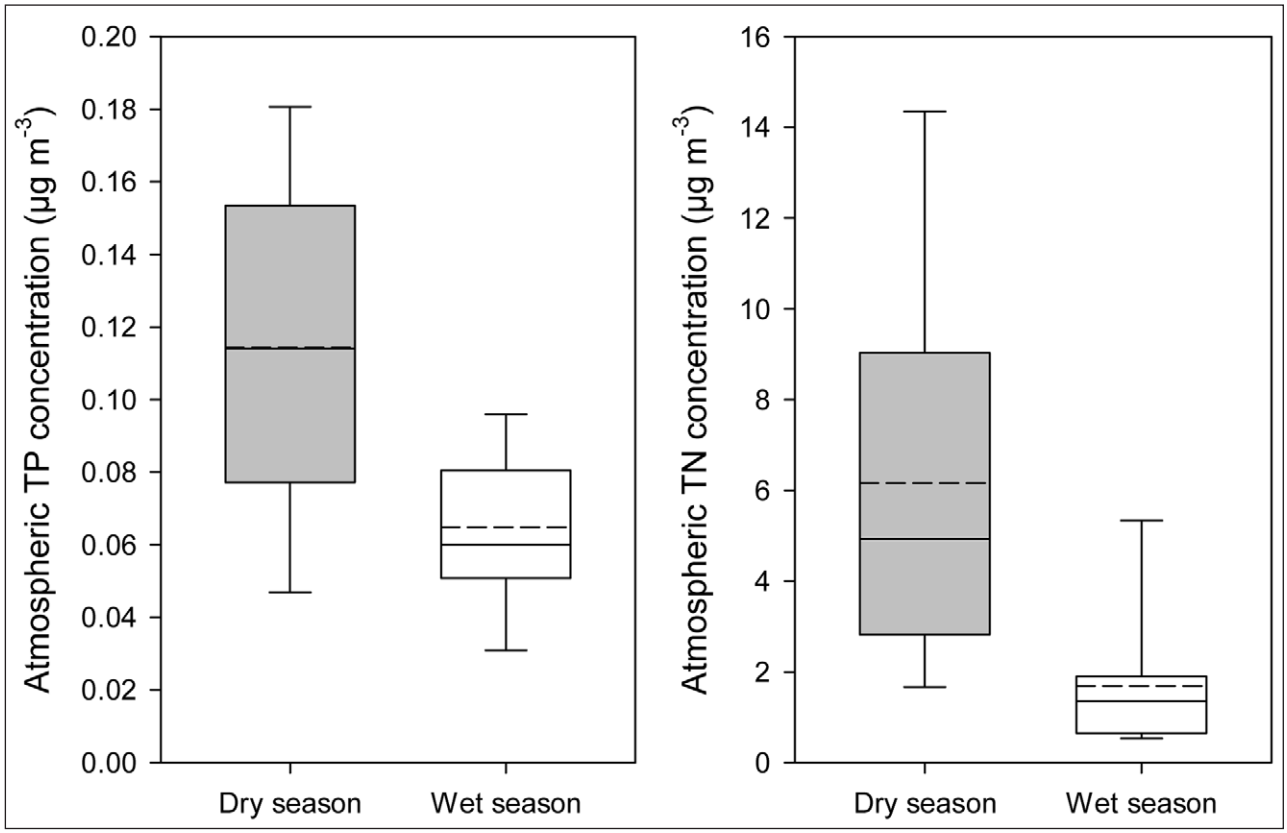

Figure 6: Concentrations of atmospheric total nitrogen and total phosphorus. Seasonal variations of atmospheric total nitrogen (TN) and phosphorus (TP) concentrations in PM_{10}. Box-and-whisker plots show median (straight line) and average (dashed line) concentrations. Note different scales for the y-axes. DOI: https://doi.org/10.1525/elementa.255.f6

aerosols during the dry season might be a source of N and P to the sea surface.

3.2. Seasonal variations of salinity

The seasonal variations of salinity in Halong Bay were characterized by a strong decrease during the wet season driven by the input of freshwater from the watershed on the northern part of the Bay (**Figure 7**). This input of freshwater resulted in a marked salinity gradient from 03 May to 05 September 2013, expanding from stations A to D. The total volume of freshwater coming from the watershed of the Cua Luc Bay during the wet season was about 1.7×10^9 m^3 (weekly average ~0.1×10^9 m^3). A slight decrease in salinity was also observed in December 2012, subsequent to the heavy rainfalls that occurred during this period (**Figure 3**).

3.3. Chlorophyll a concentrations

The seasonal distribution of Chlorophyll *a* concentration in ULW was characterized by a moderate bloom from the end of November 2012 to end of January 2013 (up to 6 μg Chl *a* L^{-1} at station A on 18 January), followed by a more pronounced bloom from mid-May 2013 to mid-August 2013 (up to 11 μg Chl *a* L^{-1} at station C on 10 August) (**Figure 8**). Both blooms started at station A and gradually developed towards the more oceanic stations. The seasonal distribution of Chl *a* concentration in the SML largely followed that observed in ULW, except for the early development of the bloom in the SML in October–November 2012. The Chl *a* concentration during this bloom reached values of 14 to 30 μg Chl *a* L^{-1} in the SML, and were 8 to 17 times higher than those observed in ULW during the same period. The highest Chl *a* concentration measured in the SML during the second bloom (14 μg Chl *a* L^{-1} on 10 August) was similar to that observed in ULW. Apart from the bloom observed in the SML in October–November 2012, the SML was not particularly enriched in Chl *a* in comparison with ULW (average EF_{Chla} = 1.0 ± 0.7, n = 48). These two blooms occurred during the periods of salinity decrease (**Figure 7**), suggesting that they were initiated and sustained by nutrient loads associated with freshwater runoff.

3.4. Seasonal variations of inorganic and organic nutrient concentrations

The concentrations of DIN and DON in ULW varied between 0.7 and 31.4 μmol L^{-1} and between 6.4 and 35.6 μmol L^{-1}, respectively (**Figure 9**). The concentrations of DIN and DON in the SML varied between 1.0 and 61.0 μmol L^{-1} and between 4.9 and 38.0 μmol L^{-1}, respectively (**Figure 9**).

The seasonal variations of DIN were similar in the SML and ULW, and characterized by a gradient of decreasing concentration expanding from stations A to D that developed from the beginning to the end of the wet season. The similarity observed for the variations of DIN in the SML and ULW suggests that these two layers were subjected to similar enrichment processes; i.e., a DIN-enrichment associated with freshwater runoff. However, during the first decrease in salinity observed in December 2012 (**Figure 7**), a strong decrease in DIN concentration was observed, concomitant with the development of a phytoplankton bloom (**Figure 8**), which suggests that most of the DIN brought to the bay by the rivers may have been assimilated during primary production. A similar pattern was observed during the wet season, where DIN concentration first increased at the beginning of the wet season, but decreased during the course of the phytoplankton bloom (i.e., from 03 May to 10 August),

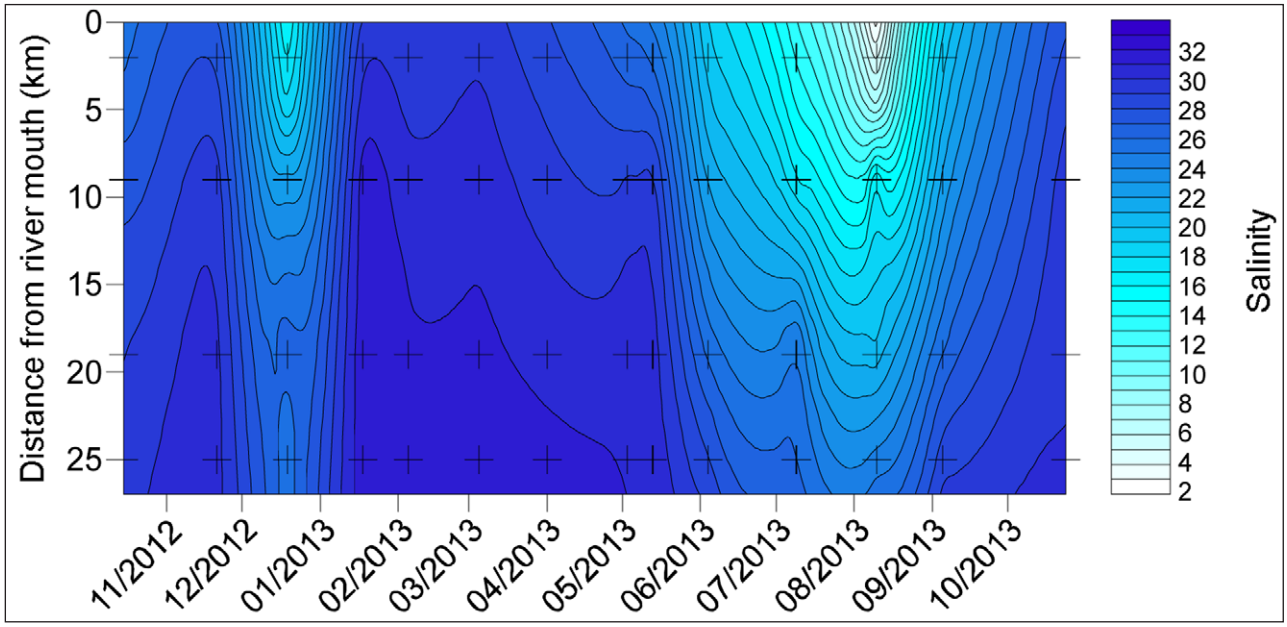

Figure 7: Salinity. Spatiotemporal variations of salinity (color scale) in ULW from October 2012 to October 2013. Each black cross represents a sampling occasion. The y-axis represents the distance from river mouth to the sampling stations; i.e., station A at 2 km, station B at 9 km, station C at 19 km, and station D at 25 km. DOI: https://doi.org/10.1525/elementa.255.f7

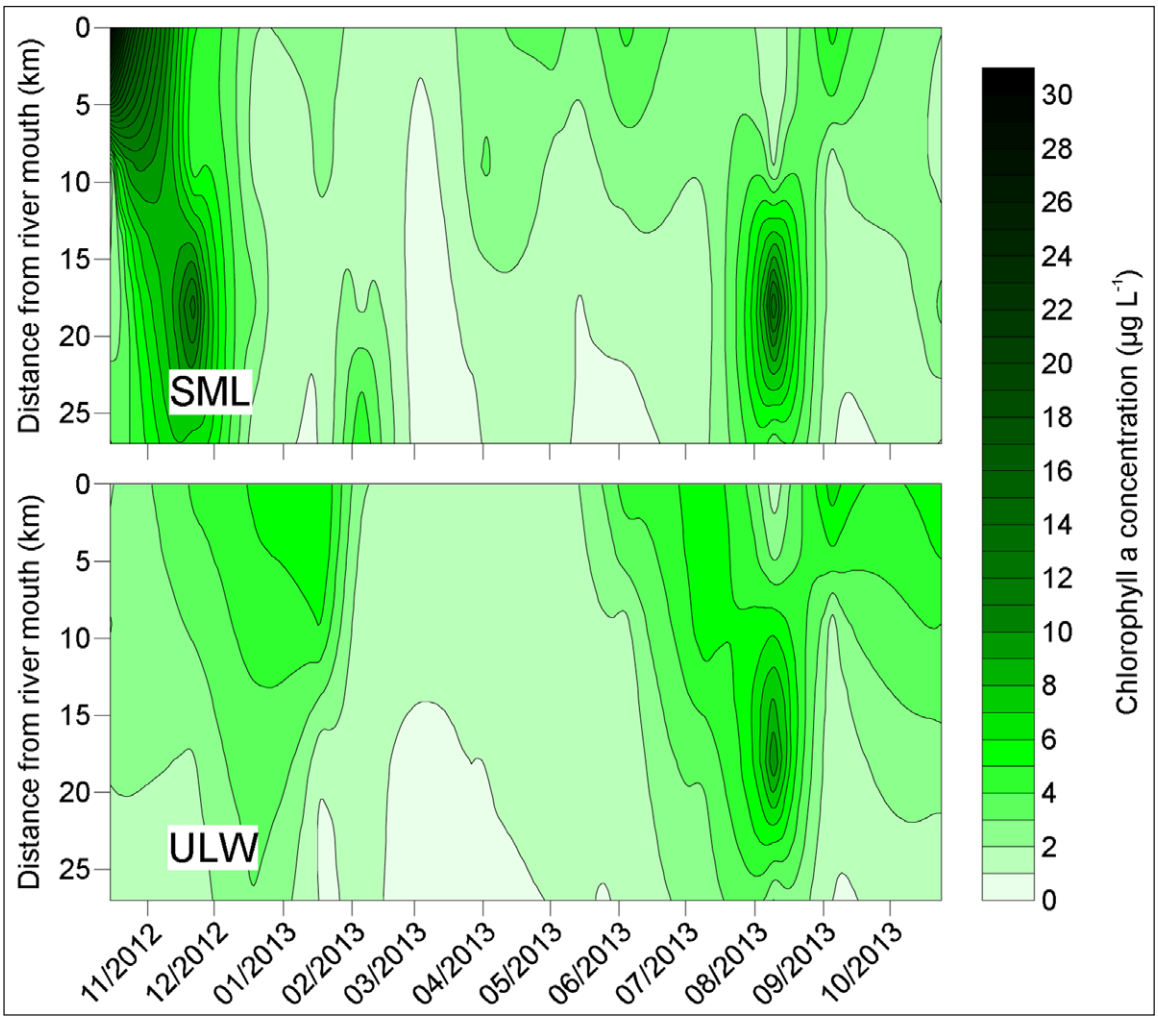

Figure 8: Concentrations of Chlorophyll *a*. Spatiotemporal variations of Chlorophyll *a* concentration (color scale) in the sea surface microlayer (SML, top panel) and underlying water (ULW, bottom panel) from October 2012 to October 2013. DOI: https://doi.org/10.1525/elementa.255.f8

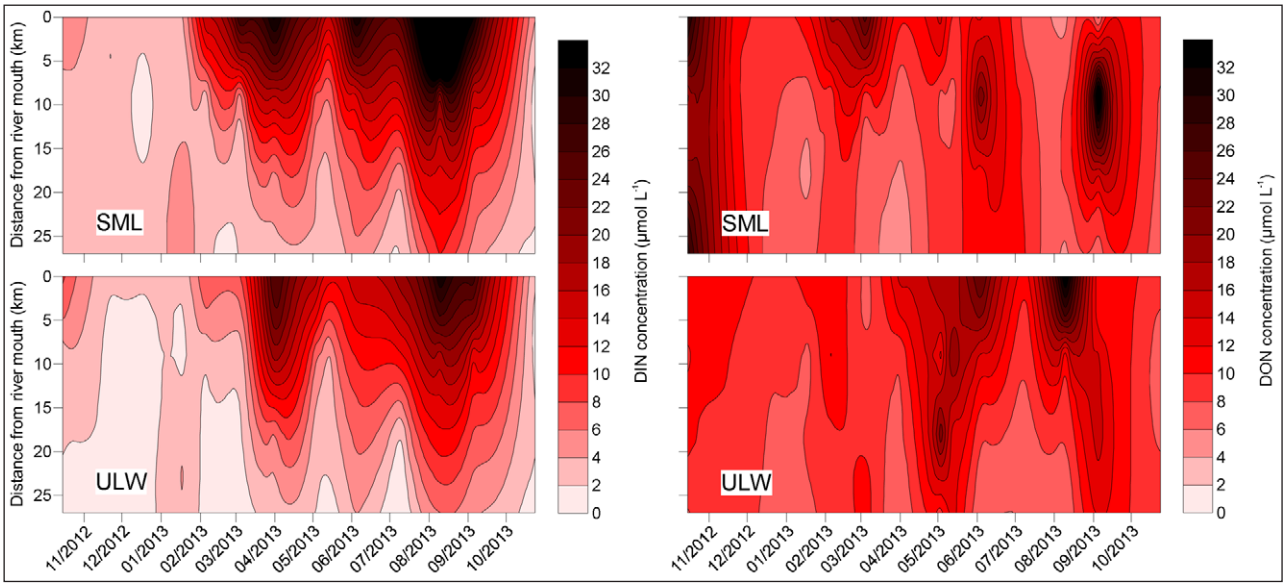

Figure 9: Concentrations of DIN and DON. Spatiotemporal variations in concentrations (color scales) of DIN (left panels) and DON (right panels) in the sea surface microlayer (SML, top panels) and in underlying water (ULW, bottom panels) from October 2012 to October 2013. Highest concentrations measured (up to 38 µm L^{-1}) exceed the scale bar. DOI: https://doi.org/10.1525/elementa.255.f9

despite massive inputs associated with freshwater runoff. The demise of the wet season bloom occurred abruptly end of August, despite high DIN input from the river, suggesting P-limitation. After the demise of the bloom, the concentration of DIN increased again until the end of the wet season. A similar seasonal pattern was observed for DON concentration in ULW (i.e., input from the river during the wet season, with uptake during the phytoplankton bloom), but no clear seasonal pattern was observed for the concentration of DON in the SML (**Figure 9**).

The concentrations of DIP and DOP in ULW varied between 0.00 and 0.33 μmol L^{-1} and between 0.04 and 0.34 μmol L^{-1}, respectively (**Figure 10**). The concentrations of DIP and DOP in the SML varied between 0.00 and 0.40 μmol L^{-1} and between 0.15 and 2.25 μmol L^{-1}, respectively (**Figure 10**). Opposite to the pattern observed for DIN, the input of freshwater during the wet season led to a strong decrease of DIP concentration in the bay, in both the SML and ULW. The observed decrease in DIP concentrations coincided with the decrease in salinity (i.e., the input of freshwater), but also with the build-up of phytoplankton biomass (**Figure 8**), hence suggesting that DIP was rapidly assimilated during primary production leading to P depletion in the bay from 03 May to 10 August.

While the concentration of DOP in ULW was relatively constant in the bay during the annual cycle (average ± SD = 0.16 ± 0.07 μmol L^{-1}, n = 56), it showed strong seasonal variations in the SML, with average concentrations (±SD) during the dry and wet seasons of 0.94 ± 0.36 μmol L^{-1} (n = 34) and 0.39 ± 0.14 μmol L^{-1} (n = 22), respectively (**Figure 10**). This seasonal pattern suggests that the deposition of aerosols during the dry season may have contributed to the enrichment of the SML in organic phosphorus.

Seasonal variations of the concentrations of DIN, DIP, DON and DOP resulted in high seasonal variations of N:P ratios, both for the inorganic and inorganic nutrients (**Figure 11**).

Halong Bay was $P_{inorganic}$-limited throughout the year, as reflected by $N:P_{inorganic}$ ratios >> 16. The $N:P_{inorganic}$ ratio averaged 125 (range of 10 to 1525, n = 56) and 182 (range of 8 to 1577, n = 56) in ULW and the SML, respectively. This limitation in DIP was even more severe during the wet season, with average $N:P_{inorganic}$ ratios reaching 298 and 381, in ULW and the SML, respectively. This seasonal trend was due to the massive input of DIN by river runoff, coupled with the assimilation of all of the available DIP during the phytoplankton bloom.

The seasonal variations of the $N:P_{organic}$ ratio differed considerably from those of the $N:P_{inorganic}$ ratio. With an annual average $N:P_{organic}$ ratio of 85 (range of 19 to 593), ULW was $P_{organic}$-limited throughout the year, but this limitation was relatively constant. In contrast, the $N:P_{organic}$ ratio in the SML showed strong seasonal variations, characterized by a limitation in DON during the dry season ($N:P_{organic}$ ratio = 11.1 ± 3.2, n = 34) followed by a limitation in DOP during the wet season ($N:P_{organic}$ ratio = 30.9 ± 11.8, n = 22).

3.5. Seasonal variations of particulate and dissolved organic and black carbon

The concentration of T-POC ranged from 9.3 to 100.4 μmol C L^{-1} and from 23.9 to 26440 μmol C L^{-1} in ULW and the SML, respectively, and the concentration of PBC ranged from 4.0 to 29.8 μmol C L^{-1} and from 8.4 to 25610.1 μmol C L^{-1} in ULW and the SML, respectively (**Figure 12**).

In ULW, the concentrations of T-POC and PBC inversely followed the decreasing salinity gradient, suggesting an input of particulate matter associated with river runoff coupled with an increase of non-PBC POC, linked to the phytoplankton bloom in summer 2013. On average, PBC contributed 40 ± 12% of the T-POC concentration (range

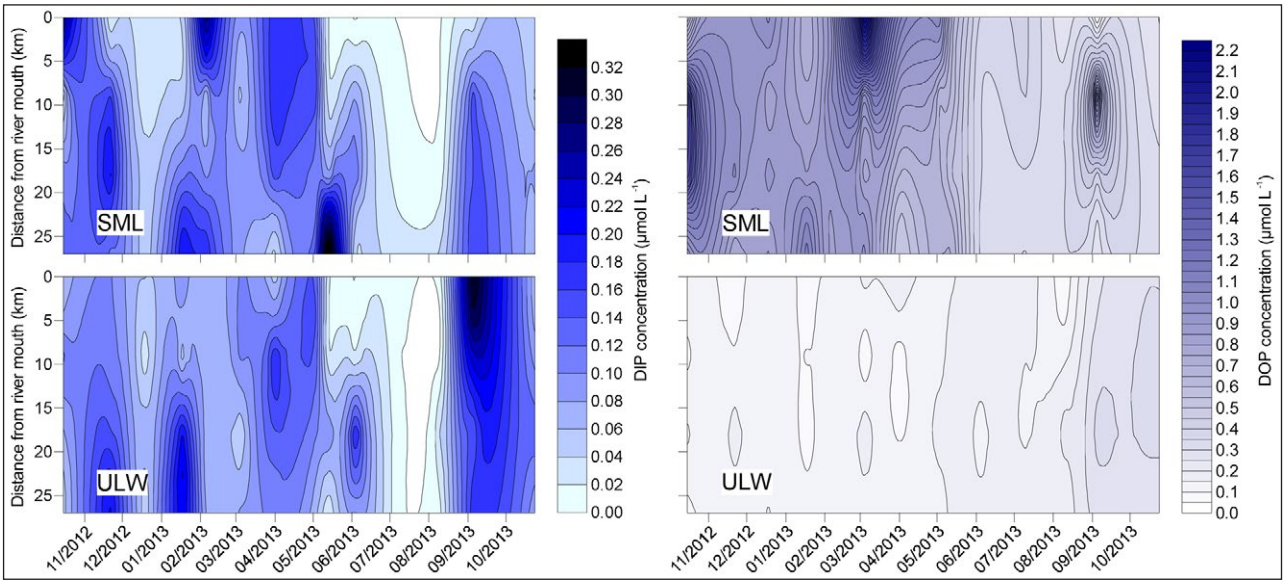

Figure 10: Concentrations of DIP and DOP. Spatiotemporal variations in concentrations of DIP (left panels) and DOP (right panels) in the SML (top panels) and ULW (bottom panels) from October 2012 to October 2013. DOI: https://doi.org/10.1525/elementa.255.f10

of 15 to 68%) in ULW, and was significantly higher during the dry season (48 ± 11%) than during the wet season (31 ± 11%) (**Figure 13**). As the concentration of PBC increased during the wet season, the observed decrease of the contribution of PBC to T-POC during this period can be attributed to the build-up of phytoplankton biomass.

In the SML, the seasonal variations of the concentrations of T-POC and PBC followed a different trend to that observed in ULW. Although highly variable, both T-POC and PBC concentrations in the SML were significantly higher (Mann-Whitney Rank Sum Test, $p < 0.001$) during the dry season (1135 ± 4999 μmol C L^{-1}, n = 26) than during the wet season (22.8 ± 14.1 μmol C L^{-1}, n = 30) (**Figure 12**). The average contribution of PBC to T-POC concentration in the SML was 47 ± 17% (range of 11 to 97%) and was not significantly different during the dry and the wet seasons (**Figure 13**).

The concentrations of T-DOC ranged from 76.6 to 132.6 μmol C L^{-1} in ULW and from 79.7 to 278.8 μmol C L^{-1} in the SML, while the concentrations of DBC ranged from

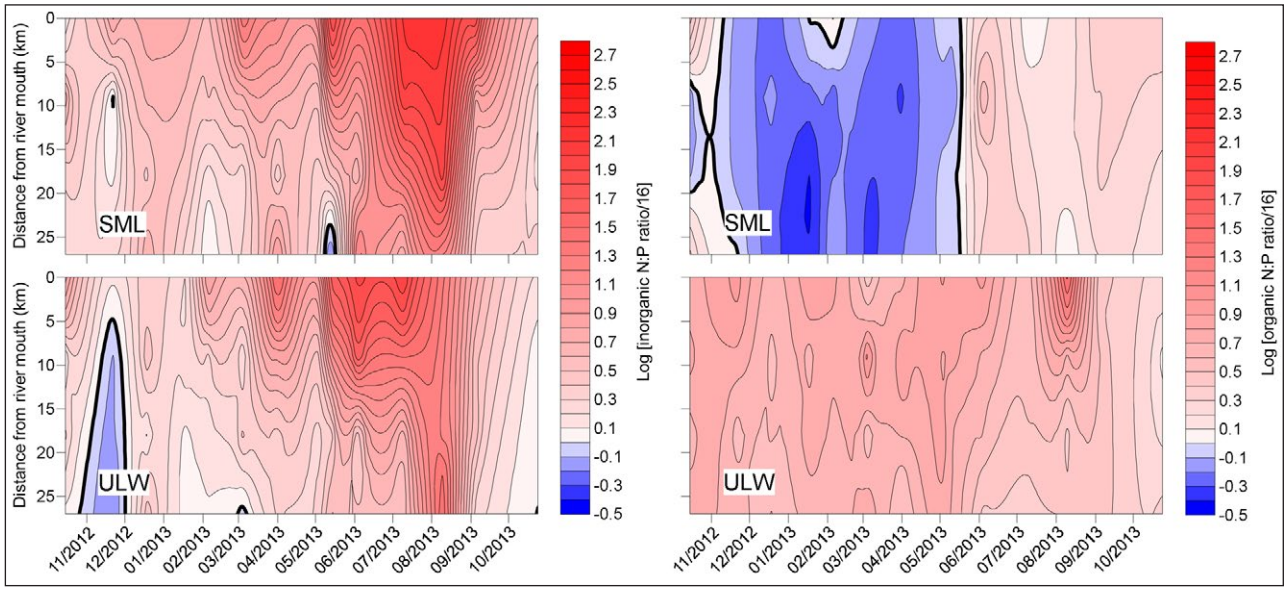

Figure 11: Normalized inorganic and organic N:P molar ratios. Spatiotemporal variations of the inorganic (left panels) and organic (right panels) N:P molar ratios normalized by the Redfield N:P ratio of 16, in the SML (top panels) and ULW (bottom panels) from October 2012 to October 2013. Due the wide range of these values, they are presented on a log scale. Negative values (blue color scale) are N:P ratios < 16; positive values (red color scale) are N:P ratios > 16. The black bold lines represent the Redfield N:P ratio of 16. DOI: https://doi.org/10.1525/elementa.255.f11

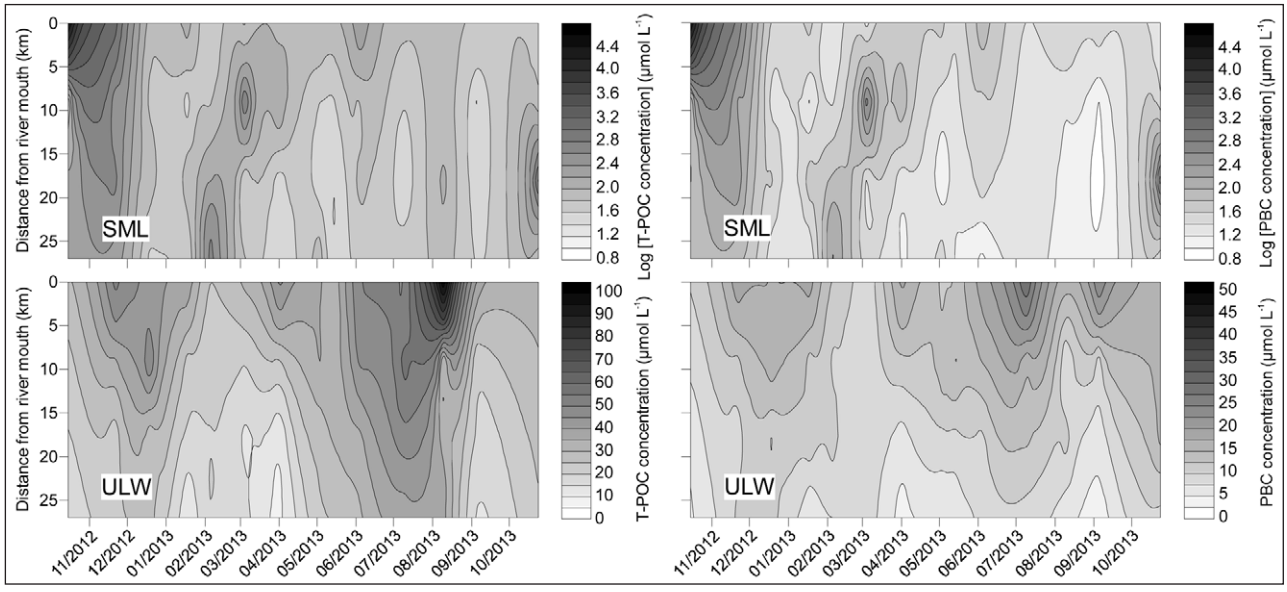

Figure 12: Concentrations of T-POC and PBC. Spatiotemporal variations of concentrations of T-POC (left panels) and PBC (right panels) in the SML (top panels) and ULW (bottom panels) from October 2012 to October 2013. Due to the wide ranges of these values in the SML, they are presented on a log scale. DOI: https://doi.org/10.1525/elementa.255.f12

1.4 to 6.5 μmol C L^{-1} in ULW and from 1.5 to 7.1 μmol C L^{-1} in the SML (**Figure 14**). The seasonal variations of T-DOC and DBC were similar in both ULW and the SML; i.e., they followed a gradient of decreasing concentration, expanding from stations A to D, during the wet season. This pattern, shared with that of T-POC and PBC concentrations (**Figure 12**), as well as DIN concentration (**Figure 9**), suggests that freshwater from river runoff was enriched in both DOC and DBC. The contribution of DBC to T-DOC concentration was very similar in ULW (from 1.6 to 5.6%; average = 2.6 ± 0.9%, n = 56) and in the SML (from 1.4 to 6.2%; average = 2.6 ± 1.1%, n = 56) and was significantly higher (Mann-Whitney Rank Sum Test, $p < 0.001$) during the wet season (3.4 ± 0.9%, n = 22) than during the dry season (2.1 ± 0.3%, n = 34) (**Figure 13**).

3.6. Enrichment of the sea surface microlayer

While neither seasonal nor spatial pattern was observed for the EF of DIP and DON (i.e., the SML was either enriched or depleted in DIP and DON independently from the season or from river runoff), the concentrations of DIN, DOP, T-POC, T-DOC, PBC and DBC were always higher in the SML than in ULW (i.e., EF > 1) (**Figure 15**). The concentrations of DIN, T-DOC and DBC were slightly

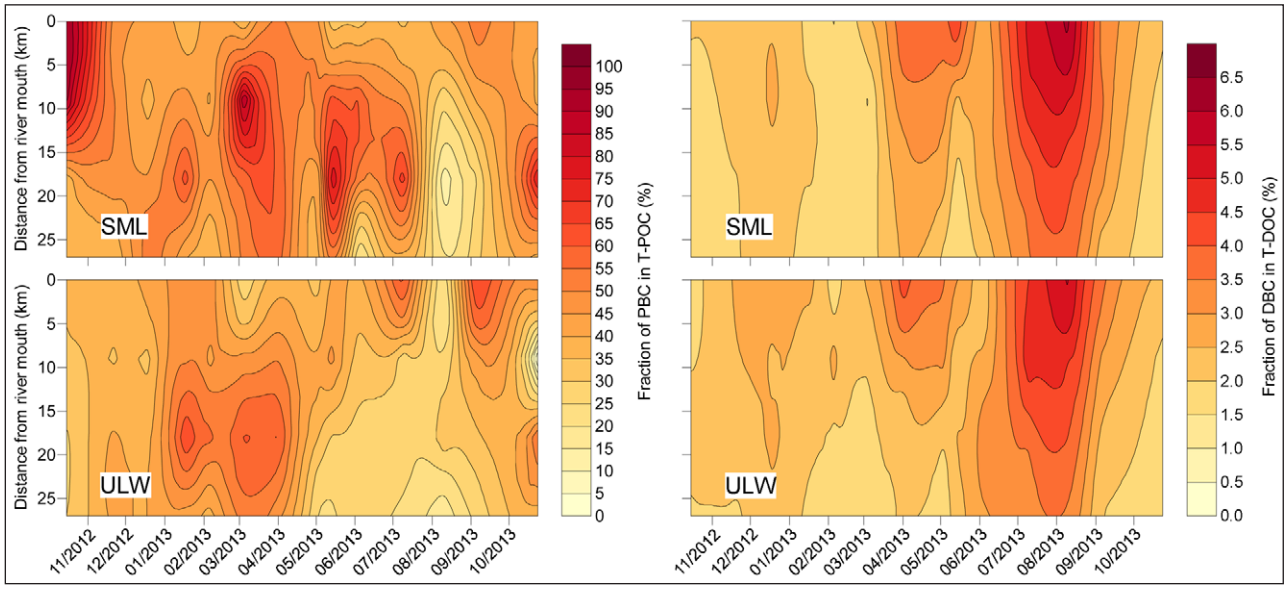

Figure 13: Contribution of BC to T-POC and T-DOC. Spatiotemporal variations of the contribution of BC to the pools of T-POC (left panels) and T-DOC (right panels), in the SML (top panels) and ULW (bottom panels) from October 2012 to October 2013. DOI: https://doi.org/10.1525/elementa.255.f13

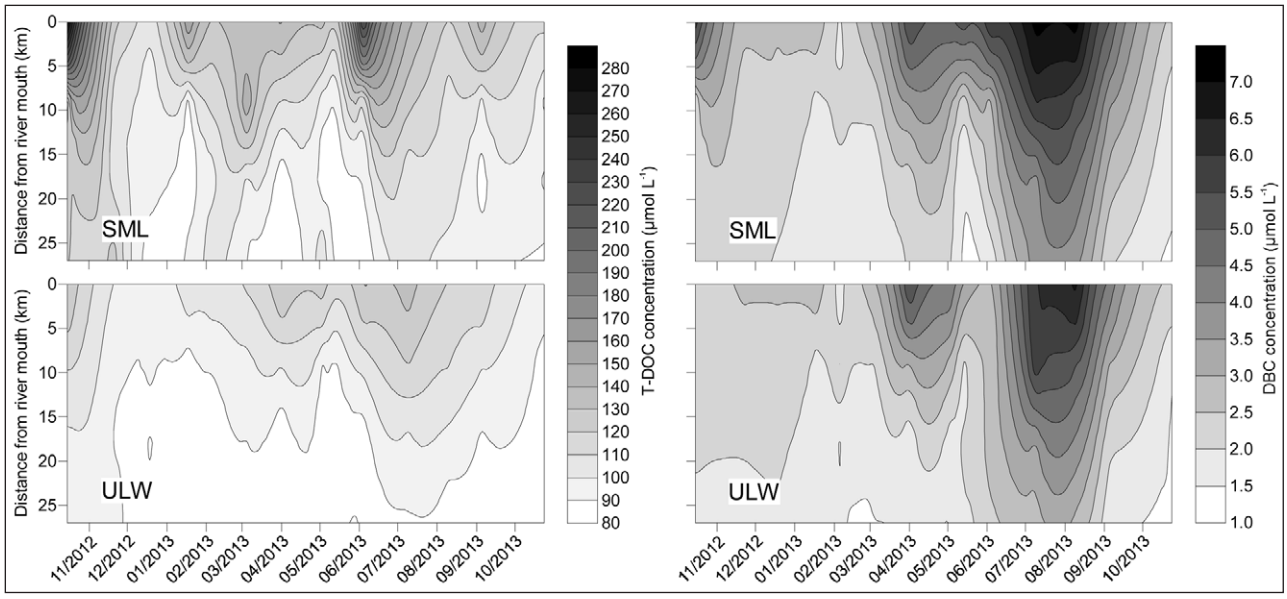

Figure 14: Concentrations of T-DOC and DBC. Spatiotemporal variations of concentrations of T-DOC (left panels) and DBC (right panels) in the SML (top panels) and ULW (bottom panels) from October 2012 to October 2013. DOI: https://doi.org/10.1525/elementa.255.f14

higher in the SML throughout the year (EF_{DIN} = 1.59 ± 0.76; $EF_{T\text{-}DOC}$ = 1.14 ± 0.21; EF_{DBC} = 1.14 ± 0.29; n = 56), and no significant seasonal or spatial pattern was observed. The SML was also enriched in DOP, T-POC and PBC throughout the year (EF_{DOP} = 5.80 ± 4.42; $EF_{T\text{-}POC}$ = 22.84 ± 126.89; EF_{PBC} = 55.01 ± 352.14; n = 56), but these enrichments were much higher during the dry season (EF_{DOP} = 8.71 ± 4.08; $EF_{T\text{-}POC}$ = 42.36 ± 175.52; EF_{PBC} = 102.37 ± 483.97, n = 30), than during the wet season (EF_{DOP} = 2.44 ± 1.34; $EF_{T\text{-}POC}$ = 1.87 ± 1.04; EF_{PBC} = 2.19 ± 1.24; n = 26).

3.7. River inputs

The input of nutrients and organic matter by river discharge during the wet season can be estimated from linear regression analyses of POC, DOC, PBC, DBC, DIN, DIP, DON and DOP concentrations as a function of salinity. The concentrations of POC, DOC, PBC, DBC and DIN in ULW, and the concentrations of DBC and DIN in the SML, were significantly correlated with salinity (**Figure 16**). The relationship between DBC and salinity was exactly the same for ULW and the SML, and hence data were combined. The Y-intercept corresponds to the concentration of each parameter at salinity = 0; i.e., in freshwater entering the Cua Luc Bay from its watershed.

The concentrations of POC, DOC, PBC, DBC and DIN in river water were estimated to be 58, 134, 26, 8 and 34 μmol L^{-1}, respectively. Variations of DIP, DON and DOP concentrations in Halong Bay during the wet season were not linked to changes in salinity, suggesting that the river system was not a major source of DIP, DON and DOP to the bay waters. Considering that the total volume of freshwater entering Halong Bay via river runoff in the Cua Luc

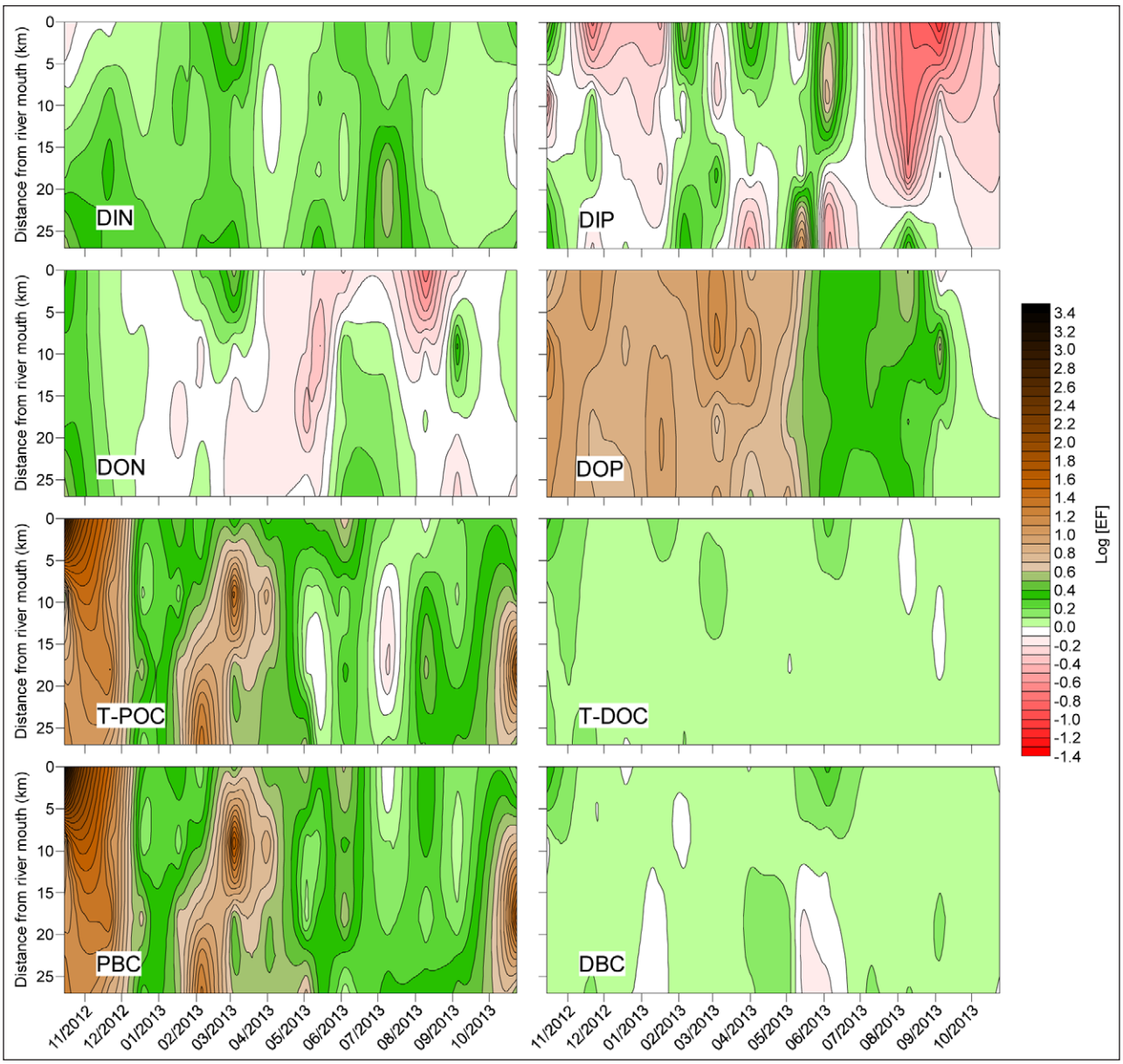

Figure 15: Enrichment factors in the SML. Spatiotemporal variations of the enrichment factors (EF) of DIN, DIP, DON, DOP, T-POC, T-DOC, PBC and DBC. Due the wide range of values for EF, they are presented on a log scale. Negative (red color scale) and positive values (green and brown color scale] of EF indicate lower and higher concentrations in the SML in comparison to ULW, respectively. DOI: https://doi.org/10.1525/elementa.255.f15

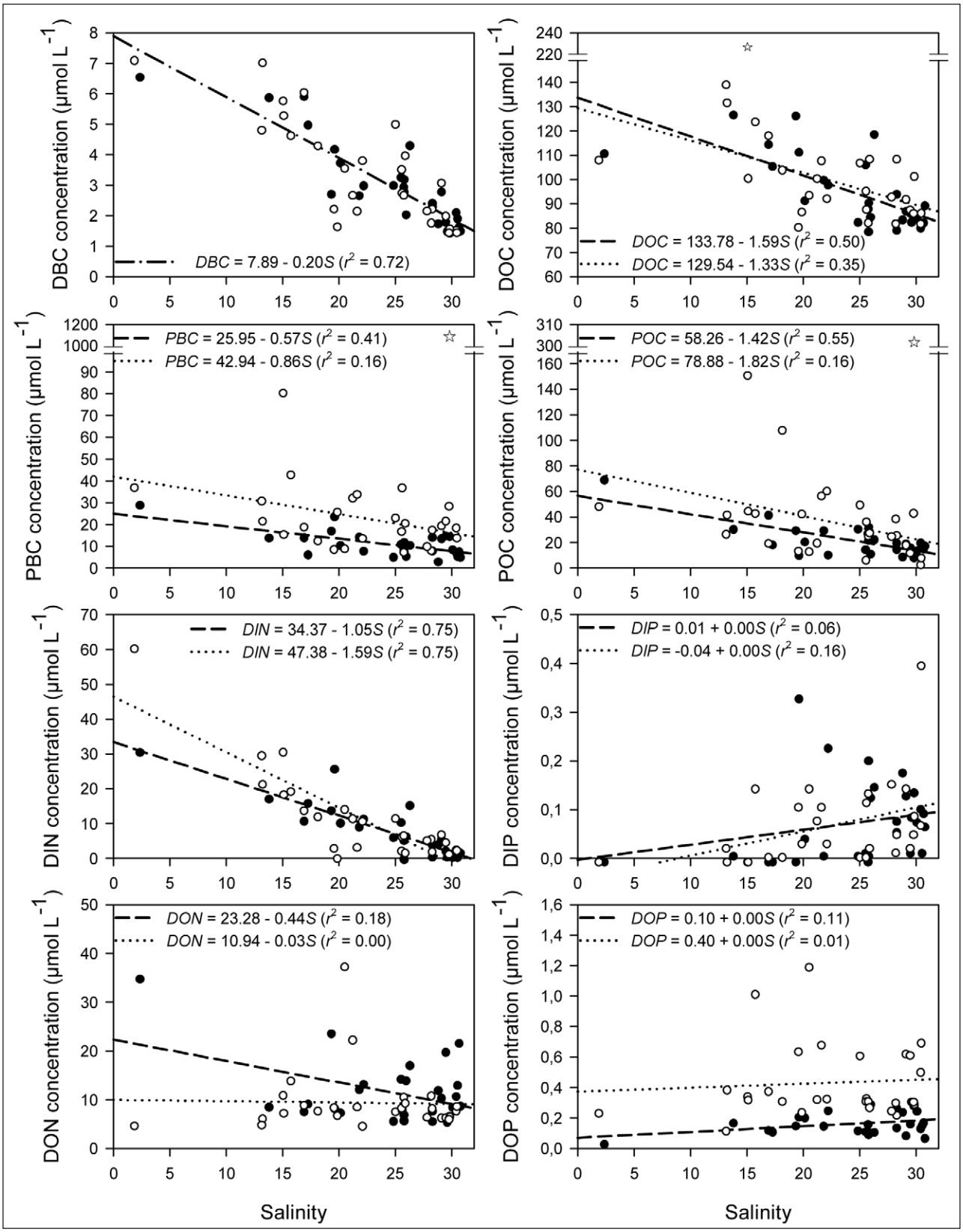

Figure 16: Linear regression analyses. Linear regression analyses of the concentrations of POC, DOC, PBC, DBC, DIN, DIP, DON and DOP, as a function of salinity during the wet season. The regression lines ($y = y_0 + aS$; where S is the salinity, y_0 is the expected concentration at salinity = 0, and a is the slope of the regression line) have been fitted to the data (n = 28) obtained during the wet season (from May to September 2013) for the SML (dotted line, closed circles) and ULW (dashed line, open circles). The relationship between DBC and salinity (upper left panel) was exactly the same for the SML and ULW, and hence data were combined (dashed-dotted line). One value from the SML (star symbol) was excluded from the regression analyses for PBC, POC and DOC. DOI: https://doi.org/10.1525/elementa.255.f16

watershed was 2.03×10^9 m^3 during the wet season (~70% of the annual river discharge), the fluxes of POC, DOC, PBC, DBC and DIN in Halong Bay during the wet season were estimated to be 118, 273, 53, 16 and 69 Mmol yr^{-1}, respectively. Assuming that the concentrations of POC, DOC, PBC, DBC and DIN in river water are similar during the dry and wet seasons, and considering an annual river discharge of 2.64×10^9 m^3, the annual fluxes of POC, DOC, PBC, DBC and DIN in Halong Bay may reach 153, 354, 69, 21 and 90 Mmol yr^{-1}, respectively.

4. Discussion

4.1. Partitioning of BC in dissolved and particulate fractions

During this first study of the seasonal variations of DBC and PBC concentrations for a complete annual cycle in Halong Bay, BC was found in significant concentrations on all sampling occasions, both in the dissolved and particulate fractions. In underlying water, the observed contribution of DBC to DOC (1.6–5.6%) is about twice that reported in previous studies for coastal DOC using the same analytical method (0.9–2.6%; Dittmar, 2008). The lower contribution of DBC to DOC reported by Dittmar (2008) is due to the lower concentration of DBC in their study region of the Gulf of Mexico (0.8–3.7 μmol C L^{-1}) compared to Halong Bay (1.4–6.5 μmol C L^{-1}).

The concentration of PBC in ULW, which averaged 11.3 ± 5.0 μmol C L^{-1} (n = 56) and contributed 39.5 ± 12.5% to the pool of POC, is more than twice as high as that reported in previous studies (Flores-Cervantes et al., 2009; Fang et al., 2016). As the concentration of POC in surface waters can be highly variable in space and time, the results reported in different studies are best compared in terms of concentration rather than relative contribution to POC. For example, the contribution of PBC to POC varied from about 15 to 68% in ULW of Halong Bay, but from undetectable to 2.7% in the western Arctic and Subarctic Oceans (Fang et al., 2016) and from about 1 to 20% in the Gulf of Maine (Flores-Cervantes et al., 2009), which suggests that Halong Bay is the most BC-impacted coastal marine system studied so far. However, comparing the concentrations of PBC measured in these different marine systems shows that the impact of PBC could be much higher than when only inferred from the contribution of PBC to POC. Indeed, the concentrations of PBC in ULW (average of 11.3 μmol C L^{-1}) were about 500 times higher than those of PBC in the western Arctic and Subarctic Oceans (average of 0.02 μmol C L^{-1}; Fang et al., 2016), and about 30 times higher those of PBC in the Gulf of Maine (average of 0.34 μmol C L^{-1}; Flores-Cervantes et al., 2009). This comparison shows that Halong Bay is a severely BC-impacted coastal ecosystem.

While this study is unique in determining the concentrations of BC in the SML, the occurrence and accumulation of polycyclic aromatic hydrocarbons (PAHs) in the SML have been reported in several studies. The SML is known to accumulate atmospheric PAHs (Cincinelli et al., 2001; Wurl and Obbard, 2004; Manodori et al., 2006; Guitart et al., 2007; Lim et al., 2007; Stortini et al., 2009). Because PAHs are intrinsic to the composition of BC (Akhter et al., 1984, 1985; Sergides et al., 1987), the high concentration of PAHs observed in the SML is consistent with BC being enriched at the air-sea interface. The concentration of PBC in the SML varied between 8 and 25610 μmol C L^{-1} during the annual cycle, and was highly variable (539 ± 3416 μmol C L^{-1}, n = 56). The high variability observed for the concentration of PBC (as well as for POC) in the SML may be caused by surface currents concentrating and isolating patches of highly BC-enriched SML. In some occasions, the concentration of PBC in the SML was so high that it appeared as black slicks extending over large surface areas, and the SML samples collected were totally black (**Figure 2**). These black slicks were commonly observed during the dry season.

4.2. Seasonal dynamics (atmospheric versus river inputs)

Halong Bay is affected by winter monsoon, characterized by low precipitation and weak northeastern winds dominating from October to May, alternating with summer monsoon, characterized by high precipitation and strong southeastern winds dominating from May to October. The monsoon regime affects the concentration of atmospheric BC, with high and low concentrations during the dry and wet seasons, respectively (Hien et al., 2002; Cohen et al., 2010; B Guinot, personal communication). This monsoon regime controls the input of BC and of other biogeochemical variables to Halong Bay, by favoring dry deposition of atmospheric BC originating from the north during the dry season, and favoring wet deposition and river discharge during the wet season.

The seasonal pattern for the EF of DOP, T-POC and PBC suggests that the composition of the SML is strongly impacted by dry deposition of aerosols, which should be higher during the dry season considering the observed high concentrations of atmospheric BC, OC, TN, and TP (**Figures 5** and **6**). However, the fact that EF of DIN, T-DOC and DBC did not show seasonal trends (i.e., no increase during the dry season) suggests that these parameters were not affected by seasonal variations of aerosol deposition and that their concentrations were driven by the same processes in ULW and the SML. In this context, the observed moderate enrichment of the SML in DIN, T-DOC and DBC could be due to a mechanism favoring their ascent toward the SML (e.g., association with ascending particles).

During the dry season, the SML was particularly enriched in DOP, POC and PBC compared to ULW (**Figure 15**). This enrichment suggests that the SML was strongly impacted by dry deposition of carbonaceous aerosols. The DOP-enrichment of the SML during the dry season may be due to the deposition of organic phosphorus from natural terrestrial or anthropogenic sources (e.g., combustion of biomass and fossil fuels, and windblown fertilizer or organophosphorus pesticides) that were associated with atmospheric BC. Such phosphorus-containing organic compounds associated with anthropogenic aerosols are highly soluble and may be released in seawater as DOP (Anderson et al., 2010), hence fueling new oceanic production in this P-limited marine system. Interestingly,

the Gulf of Tonkin has been identified as one of the few hotspots of 'new' soluble organic phosphorus deposition to the ocean from anthropogenic and natural terrestrial sources (Kanakidou et al., 2012). As evidenced by the seasonal changes of the $N:P_{organic}$ ratio in the SML (**Figure 11**), this significant input of organic phosphorus in the SML coinciding with the input of PBC during the dry season was sufficient to relieve the P-limitation with organic phosphorus, which may have stimulated heterotrophic activity in the SML. Contrary to PBC and POC, the concentrations of DBC and DOC did not increase in the SML during the dry season. This contrast suggests that atmospheric BC, which was deposited at the sea surface, did not solubilize or release DBC.

During the wet season, Halong Bay was largely impacted by river inputs, as evidenced by the spatial and seasonal distributions of several parameters that followed salinity. Although the concentration of DBC and its contribution to the pool of DOC did not vary much during the annual cycle, a clear seasonal pattern was observed. The spatial and seasonal distributions of DBC followed that of salinity in the bay, and declined along the increasing salinity gradient. The spatial and seasonal distributions of DBC in Halong Bay suggest that riverine runoff that occurred during the wet season was efficient in mobilizing and transporting DBC to the ocean. Previous studies have reported a similar relation between salinity and the concentration of DBC (Mitra et al., 2002; Mannino and Harvey, 2004; Marques et al., 2017), with global estimates indicating that the riverine DOC pool, of which about 10% is DBC, provides an input pathway that brings about 26 Tg DBC yr^{-1} to the ocean (Jaffé et al., 2013). The high contribution of DBC to the pool of T-DOC in riverine flux reported in previous studies (Jaffé et al., 2013; Stubbins et al., 2015; Wang et al., 2016) is confirmed for the river system converging in Cua Luc Bay by the observed gradient of increasing DBC fraction toward the river and the high contribution of DBC to the pool of DOC (> 6% at station A) during the wet season, and by the high concentration of DBC at salinity = 0 estimated by regression analysis (about 8 μmol C L^{-1}; **Figure 16**). The fact that the relationship between DBC and salinity was the same for ULW and the SML (**Figure 16**), and that similar seasonal variations were observed for DBC concentrations in ULW and the SML (**Figure 14**), indicates that the concentration of DBC in ULW and the SML are governed by the same mechanism; i.e., input from the river system followed by dilution in Halong Bay.

The seasonal variations of PBC and POC concentrations in ULW followed that of DBC and DOC (**Figures 12** and **14**), hence suggesting that river runoff during the wet season was also efficient in transporting PBC that had deposited and accumulated on land during the dry season. Because DBC and PBC were measured following different analytical methods, the similar seasonal variations of DBC and PBC in ULW of Halong Bay can be considered as evidence of the robustness of each of these methods to measure the concentrations of BC in its different phases. Based on our estimates of river inputs of PBC and DBC (69 and 21 Mmol C yr^{-1}, respectively), the annual river flux of PBC was 3.8 times higher than that of DBC, which is similar to the high PBC/DBC flux ratios observed for the Yangtze and Huanghe rivers (Wang et al., 2016). The estimated concentration of PBC in river water flowing into the Cua Luc Bay during the wet season (26 μmol C L^{-1}) is equivalent to that of PBC discharge in the Mekong River (about 23 μmol C L^{-1}; calculated for each river from the annual water and PBC discharge reported in Table 9.3 of Mitra et al., 2014).

Besides DBC, DOC, PBC and POC, river runoff also brought large amounts of dissolved N compounds to the ocean during the wet season, hence contributing to the severe inorganic P-limitation in the Bay. This seasonal input of dissolved nitrogenous compounds in Halong Bay could be linked to agricultural, industrial and domestic loadings from the watershed of the Cua Luc Bay. Such input of N compounds has been described in the Red River Delta (Le et al., 2005). At the peak of the wet season, when the freshwater discharge was highest, P-limitation in ULW was extremely severe at the mouth of the Cua Luc Bay ($N:P_{inorganic}$ ratio > 1500), suggesting that agricultural, industrial and domestic practices in the watershed of the Cua Luc Bay provoke severe seasonal nutrient imbalance in Halong Bay.

Considering that the lifetime of DBC in the ocean exceeds millennia (Dittmar and Paeng, 2009; Ziolkowski and Druffel, 2010), it can be used as a conservative parameter in order to determine the dilution coefficient of the freshwater entering the Cua Luc Bay from its watershed. As a result, the dilution coefficient should be –0.2 (i.e., slope of the DBC versus salinity relationship; **Figure 16**). Subtracting this DBC-based dilution coefficient, a_{DBC}, with the slopes of other variables allows estimating their involvement in processes other than dilution. Based on these non-dilution removal slopes, the observed decreases in ULW of the concentrations of PBC, POC, DOC and DIN due to processes other than dilution of the freshwater plume were 1.9 (a_{PBC}/a_{DBC}), 6.1 (a_{POC}/a_{DBC}), 7.0 (a_{DOC}/a_{DBC}), and 4.3 (a_{DIN}/a_{DBC}) higher than explained by dilution, respectively. This exercise suggests that PBC may be three times less involved than non-pyrogenic POC in marine processes. As particulate matter can be involved in physical (e.g., sedimentation) and biological processes (e.g., remineralization), and PBC and non-pyrogenic POC are probably involved in the same physical processes as they combine into marine aggregates (Mari et al., 2014), this discrepancy suggests that PBC is less subjected to bacterial degradation and is mostly removed by sedimentation. In addition, this exercise shows that DIN and non-pyrogenic DOC concentrations decrease, respectively, 7.0 and 4.3 times faster than explained by dilution, and hence are rapidly processed in Halong Bay.

4.3. Potential consequences of high PBC concentration in Halong Bay

Owing to their highly porous structure (up to 300 m^2 g^{-1}; Zerda et al., 1999; Rockne et al., 2000) and the surface coverage with oxygen-containing functional groups (e.g., Masiello, 2004; Smith and Chughtai, 1995), BC is highly surface-active and has very high exchangeable cation sorption and retention capacity (Liang et al., 2006). Although atmospheric BC is highly aromatic and hydrophobic at formation, reactions with ozone and

other atmospheric oxidants create hydrophilic carboxylic acid groups on its exterior. In other words, although less reactive than activated carbon, PBC may act as activated carbon-like particles in seawater. Therefore, owing to its high porosity, and sorption and retention capacity, PBC is expected to have high sorptive properties for a wide variety of dissolved compounds in seawater.

While the sorptive properties of PBC in seawater have not been studied in detail yet, there is a plethora of indirect evidence that BC may efficiently adsorb a wide variety of dissolved compounds. For example, coal fly ash, which contains from 20 to 60% BC (Külaots et al., 2003, 2004; Styszko-Grochowiak et al., 2004), is very efficient at adsorbing molecules from aqueous solutions and flue gas (Baltrus et al., 2001; Külaots et al., 2004; Styszko-Grochowiak et al., 2004; Wang and Wu, 2006; Ahmaruzzaman, 2010), with adsorbing capacity largely linked to its carbon (BC) content (Hassett and Eylands, 1999; Hower et al., 2000, 2010; Külaots et al., 2003, 2004). This byproduct of coal combustion is used as a low-cost adsorbent for cleaning flue gas from SOx, NOx, mercury and organics (Bossan et al., 1995; Seigneur et al., 1998), but also for cleaning wastewater from dissolved organic matter, heavy metals, pesticides and nutrients (Gupta et al., 2002). Finally, coal fly ash has received great attention in recent years as a potential material for phosphate removal from polluted effluents, as it is easily available and cost-effective (e.g., Gray and Schwab, 1993; Ugurlu and Salman, 1998; Cheung and Venkitachalam, 2000; Grubb et al., 2000; Agyei and Strydom, 2002; Yildiz, 2004; Oguz, 2005; Chen et al., 2007). In addition, PBC in sediment has been shown to adsorb organic compounds very efficiently (Cornelissen et al., 2005; Koelmans et al., 2006). The above indirect evidence strongly supports the idea of an efficient adsorption of dissolved compounds by PBC in marine systems. This mechanism may constitute a nutrient-netting causing a nutrient-shunt, moving nutrients (C as well as inorganic and organic nutrients) from the dissolved to the particulate fractions. For example, this mechanism may remove phosphate from solution, hence increasing P-limitation in Halong Bay.

In addition, sorptive properties of PBC for DOC may lead to enhanced aggregation processes. During a field study in a lagoon of New Caledonia, Mari et al. (2014) observed a significant decrease of DOC concentration by about 6%, concomitant with a major increase (by a factor of 30) in the volume concentration of suspended particles in the water column subsequent to a massive dry deposition of atmospheric BC. Their field observations were confirmed during laboratory studies showing that a BC-enrichment event stimulated aggregation processes and removed DOC from solution. According to this scheme, the DOC-to-POC balance in a pelagic system could be affected by the concentration of PBC. In order to test this hypothesis, we estimated the POC/DOC ratio as a function of PBC concentration. The efficiency of the transfer of organic matter from the dissolved to the particulate phase via adsorption/aggregation processes, indicating the physicochemical reactivity of organic matter, can be approached by the POC/DOC ratio, which gives an indication of the aggregation efficiency (Mari et al., 2007); i.e., a high POC/DOC ratio suggests high aggregation and thus an efficient transfer of organic matter from the dissolved to the particulate phase. In order to determine the impact of PBC on the DOC-to-POC balance in Halong Bay, the POC/DOC ratio was calculated as $[(T\text{-}POC) - (PBC)]/[(T\text{-}DOC) - (DBC)]$, excluding PBC and DBC. The POC/DOC ratio as a function of PBC concentration was fitted to a power law relationship, $[POC/DOC] = a\,[PBC]^b$, where a and b are constants (**Figure**

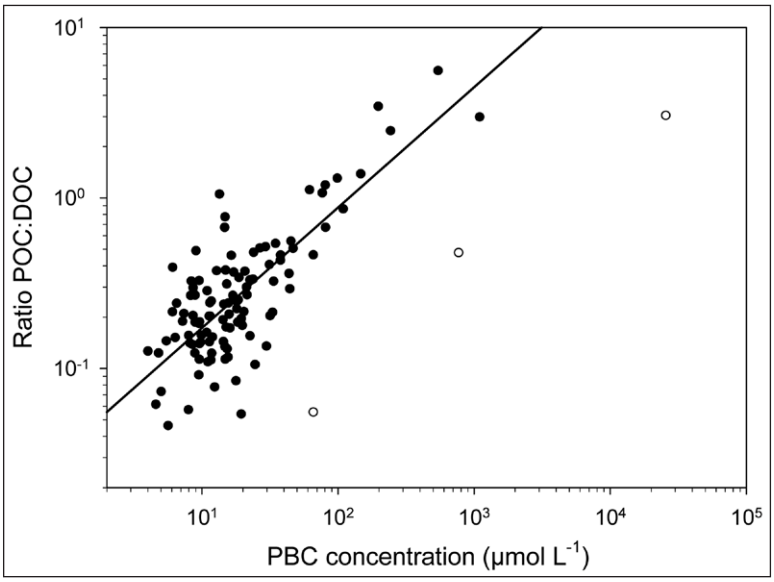

Figure 17: Impact of PBC concentration on the DOC-to-POC balance. Potential impact of PBC concentration on the DOC-to-POC balance, as represented by the POC/DOC ratio. The POC/DOC ratio was calculated as $[(T\text{-}POC) - (PBC)]/[(T\text{-}DOC) - (DBC)]$, excluding PBC and DBC. The POC/DOC ratio as a function of PBC concentration was fitted to a power law relationship, $[POC/DOC] = a\,[PBC]^b$, where a and b are constants. The measured POC/DOC ratios and PBC concentrations were plotted in log-log coordinates to obtain a and b. The three values represented by open circles, were excluded from the regression analysis. DOI: https://doi.org/10.1525/elementa.255.f17

17). During our study, the POC/DOC ratio was positively correlated with PBC concentration independent of the season ($[POC/DOC] = 0.034\ [PBC]^{0.706}$; $r^2 = 0.61$). This result suggests that the introduction of PBC to the water column of Halong Bay may enhance the transfer of organic carbon from the dissolved to the particulate phase. This enhanced transfer may be caused by the adsorption of DOC onto PBC and by the stimulation of aggregation processes due to the presence of PBC. Although such impact of PBC on the DOC-to-POC balance supports the conclusion of Mari et al. (2014), it needs to be taken with caution because it assumes that the dissolved-to-particulate continuum is largely shaped by aggregation processes, and hence does not distinguish between organic aggregates and organisms within the POC pool.

5. Conclusion

Our study shows that BC can be highly enriched in coastal systems located in regions experiencing high atmospheric BC concentrations, as in North Vietnam. This spatio-temporal study allowed to highlight the alternation of two routes for the entry of BC into the bay, each controlled by the monsoon regime: (1) a dry season route of dry atmospheric deposition through the SML resulting in a strong enrichment of the SML with PBC (as well as POC and DOP); and (2) a wet season route by riverine runoff resulting in the establishment of a gradient of decreasing concentrations of PBC and DBC (as well as DOC, POC, DIN). This seasonal dynamic could be a general pattern in coastal systems of the BC-impacted Asia-Pacific region. Considering the high concentrations observed for PBC, its high contribution to the pool of T-POC, the reported impacts of BC on microbial processes and particle dynamics, and the predicted increase on atmospheric BC concentration in the Asia-Pacific region in the coming decades, it appears urgent to better describe the fate of PBC and DBC in BC-impacted coastal systems, and the impact of BC on element cycling and marine processes and ecosystems.

Data accessibility statement

All data used in this study are available from the corresponding author upon request.

Acknowledgements

We thank Ina Ulber for help with BPCA analysis.

Funding information

This work was supported by the French National Institute of Sciences of the Universe (Project SOOT-EC2CO 2013) (to XM), the French-Vietnamese Hubert Curien Partnership (Contract No. 23971TK) (to XM), the Ministry of Science and Technology of Vietnam (Contract No. 46/2012/HD-NDT) (to TCV) and the French Research Institute for Development (IRD) (to XM).

Competing interests

The authors have no competing interests to declare.

Author Contributions

- Contributed to conception and design: XM, TCV, BG
- Contributed to acquisition of data: XM, TCV, BG, JB, J-PL, PR, JN
- Contributed to analysis and interpretation of data: XM, TCV, BG, J-PL, PR, JN, TD
- Drafted and/or revised the article: XM, TCV, BG, J-PL, PR, JN, TD
- Approved the submitted version for publication: XM, TCV, BG, JB, J-PL, PR, JN, TD

References

Agyei, NM and **Strydom, CA** 2002 The removal of phosphate ions from aqueous solution by fly ash, slag, ordinary Portland cement and related blends. *Cem Concr Res* **32**: 1889–1897, DOI: https://doi.org/10.1016/S0008-8846(02)00888-8

Ahmaruzzaman, M 2010 A review on the utilization of fly ash. *Prog Energ Combust* **36**: 327–363, DOI: https://doi.org/10.1016/j.pecs.2009.11.003

Aminot, A and **Kérouel, R** 2007 Dosage automatique des nutriments dans les eaux marines: méthodes en flux continu, edited by: IFREMER, Méthodes d'analyse en milieu marin, 188.

Anderson, LD, Faul, KL and **Paytan, A** 2010 Phosphorus associations in aerosols: What can they tell us about P bioavailability? *Mar Chem* **120**: 4456, DOI: https://doi.org/10.1016/j.marchem.2009.04.008

Baltrus, JP, Wells, AW, Fauth, DJ, Diehl, JR and **White, CM** 2001 Characterization of carbon concentrates from coal-combustion fly ash. *Energ Fuel* **15**(2): 455–462, DOI: https://doi.org/10.1021/ef000201o

Bond, TC, Doherty, SJ, Fahey, DW, Forster, PM, Berntsen, T, DeAngelo, BJ, Flanner, MG, Ghan, S, Kärcher, B, Koch, D, Kinne, S, Kondo, Y, Quinn, PK, Sarofim, MC, Schultz, MG, Schulz, M, Venkataraman, C, Zhang, H, Zhang, S, Bellouin, N, Guttikunda, SK, Hopke, PK, Jacobson, MZ, Kaiser, JW, Klimont, Z, Lohmann, U, Schwarz, JP, Shindell, D, Storelvmo, T, Warren, SG and **Zender, CS** 2013 Bounding the role of black carbon in the climate system: A scientific assessment. *J Geophys Res* **118**(11): 5380–5552, DOI: https://doi.org/10.1002/jgrd.50171

Bossan, D, Wortham, H and **Masclet, P** 1995 Atmospheric transport of pesticides adsorbed on aerosols: I. Photodegradation in simulated atmosphere. *Chemosphere* **30**: 21–29, DOI: https://doi.org/10.1016/0045-6535(94)00372-2

Cachier, H, Bremond, MP and **Buat-Menard, P** 1989 Determination of atmospheric soot carbon with a simple thermal method. *Tellus* **41**(B): 379–390. DOI: https://doi.org/10.1111/j.1600-0889.1989.tb00316.x

Chen, J, Kong, H, Wu, D, Chen, X, Zhang, D and **Sun, Z** 2007 Phosphate immobilization from aqueous solution by fly ashes in relation to their composition. *J Hazard Mater* **B139**: 293–300. DOI: https://doi.org/10.1016/j.jhazmat.2006.06.034

Cheung, KC and **Venkitachalam, TH** 2000 Improving phosphate removal of sand infiltration system using alkaline fly ash. *Chemosphere* **41**: 243–249. DOI: https://doi.org/10.1016/S0045-6535(99)00417-8

Cincinelli, A, Stortini, AM, Perugini, M, Checchini, L and **Lepri, L** 2001 Organic pollutants in sea-surface microlayer and aerosol in the coastal environment of Leghorn—(Tyrrhenian Sea). *Mar Chem* **76**: 77–98. DOI: https://doi.org/10.1016/S0304-4203(01)00049-4

Cohen, DD, Crawford, J, Stelcer, E and **Vuong, TB** 2010 Long range transport of fine particle windblown soils and coal fired power station emissions into Hanoi between 2001 to 2008. *Atmos Environ* **44**(31): 3761–3769. DOI: https://doi.org/10.1016/j.atmosenv.2010.06.047

Corbett, JJ, Winebrake, JJ, Green, EH, Kasibhatla, P, Eyring, V and **Lauer, A** 2007 Mortality from ship emissions: A global assessment. *Environ Sci Technol* **41**(24): 8512–8518. DOI: https://doi.org/10.1021/es071686z

Cornelissen, G, Gustafsson, Ö, Bucheli, TD, Jonker, MTO, Koelmans, AA and **Van Noort, PCM** 2005 Extensive sorption of organic compounds to black carbon, coal, and kerogen in sediments and soils: Mechanisms and consequences for distribution. *Environ Sci Technol* **39**(18): 6881–6895. DOI: https://doi.org/10.1021/es050191b

Daniel, A, Kérouel, R and **Aminot, A** 2005 Pasteurization: A reliable method for preservation of nutrient in seawater samples for inter-laboratory and field applications. *Mar Chem* **128–129**: 57–63. DOI: https://doi.org/10.1016/j.marchem.2011.10.002

Dittmar, T 2008 The molecular level determination of black carbon in marine dissolved organic matter. *Org Geochem* **39**: 396–407. DOI: https://doi.org/10.1016/j.orggeochem.2008.01.015

Dittmar, T, Koch, BP, Hertkorn, N and **Kattner, G** 2008 A simple and efficient method for the solid-phase extraction of dissolved organic matter (SPE-DOM) from seawater. *Limnol Oceanogr: Methods* **6**: 230–235.

Dittmar, T and **Paeng, J** 2009 A heat-induced molecular signature in marine dissolved organic matter. *Nat Geosci* **2**(3): 175–179. DOI: https://doi.org/10.1038/ngeo440

Fang, Z, Yang, W, Chen, M, Zheng, M and **Hu, W** 2016 Abundance and sinking of particulate black carbon in the western Arctic and Subarctic Oceans. *Sci Rep* **6**, 29959.

Flores-Cervantes, DX, Plata, DL, MacFarlane, JK, Reddy, CM and **Gschwend, PM** 2009 Black carbon in marine particulate organic carbon: Inputs and cycling of highly recalcitrant organic carbon in the Gulf of Maine. *Mar Chem* **113**: 172–181. DOI: https://doi.org/10.1016/j.marchem.2009.01.012

Gatari, MJ, Boman, J, Wagner, A, Janhäll, S and **Isakson, J** 2006 Assessment of inorganic content of $PM_{2.5}$ particles sampled in a rural area north-east of Hanoi, Vietnam. *Sci Total Environ* **368**: 675–685. DOI: https://doi.org/10.1016/j.scitotenv.2006.04.004

Goldberg, ED 1985 Black Carbon in the environment: Properties and distribution. John Wiley & Sons, New York.

Gray, CA and **Schwab, AP** 1993 Phosphorus-fixing ability of high pH, high calcium, coal-combustion, waste materials. *Water Air Soil Pollut* **69**: 309–320. DOI: https://doi.org/10.1007/BF00478167

Grubb, DG, Guimaraes, MS and **Valencia, R** 2000 Phosphate immobilization using an acidic type F fly ash. *J Hazard Mater* **76**: 217–236. DOI: https://doi.org/10.1016/S0304-3894(00)00200-4

Guazzotti, SA, Coffee, KR and **Prather, KA** 2001 Continuous measurements of size-resolved particle chemistry during INDOEX-Intensive Field Phase 99. *J Geophys Res* **106**(D22): 28607–28628. DOI: https://doi.org/10.1029/2001JD900099

Guitart, C, García-Flor, N, Bayona, JM and **Albaigés, J** 2007 Occurrence and fate of polycyclic aromatic hydrocarbons in the coastal surface microlayer. *Mar Pollut Bull* **54**(2): 186–194. DOI: https://doi.org/10.1016/j.marpolbul.2006.10.008

Gupta, VK, Jain, CK, Ali, I, Chandra, S and **Agarwal, C** 2002 Removal of lindane and malathion from wastewater using bagasse fly ash- a sugar industry waste. *Water Res* **36**: 2483–2490. DOI: https://doi.org/10.1016/S0043-1354(01)00474-2

Gustafsson, Ö, Haghseta, F, Chan, C, MacFarlane, J and **Gschwend, PM** 1997 Quantification of the dilute sedimentary soot phase: Implications for PAH speciation and bioavailability. *Environ Sci Technol* **31**(1): 203–209. DOI: https://doi.org/10.1021/es960317s

Hadley, OL, Ramanathan, V, Carmichael, GR, Tang, Y, Corrigan, CE, Roberts, GC and **Mauger, GS** 2007 Trans-Pacific transport of black carbon and fine aerosols (D < 2.5 μm) into North America. *J Geophys Res* **112**(D05): 309. DOI: https://doi.org/10.1029/2006JD007632

Hassett, DJ and **Eylands, KE** 1999 Mercury capture on coal combustion fly ash. *Fuel* **78**: 243–248. DOI: https://doi.org/10.1016/S0016-2361(98)00150-1

Hien, PD, Bac, VT, Tham, HC, Nhan, DD and **Vinh, LD** 2002 Influence of meteorological conditions on $PM_{2.5}$ and $PM_{2.510}$ concentrations during the monsoon season in Hanoi, Vietnam. *Atmos Environ* **36**: 3473–3484. DOI: https://doi.org/10.1016/S1352-2310(02)00295-9

Hien, PD, Bac, VT and **Thinh, NTH** 2004 PMF receptor modelling of fine and coarse PM_{10} in air masses governing monsoon conditions in Hanoi, northern Vietnam. *Atmos Environ* **38**: 189–201. DOI: https://doi.org/10.1016/j.atmosenv.2003.09.064

Ho, HH, Swennen, R, Cappuyns, V, Vassilieva, E, Neyens, G, Rajabali, M and **Tran, TV** 2013 Geogene versus anthropogene origin of trace metals in sediments in Cua Luc Estuary and Ha Long Bay, Vietnam. *Estuar Coast* **36**: 203–219. DOI: https://doi.org/10.1007/s12237-012-9562-3

Holm-Hansen, O, Lorenzen, CJ, Holmes, RW and **Strickland, JDH** 1965 Fluorimetric determination of chlorophyll. *Rapp P-V Reun Cons Int Explor Mer* **30**: 3–15.

Hower, JC, Maroto-Valer, MM, Taulbee, DN and **Sakulpitakphon, T** 2000 Mercury capture by

distinct fly ash carbon forms. *Energ Fuel* **14**: 224–226. DOI: https://doi.org/10.1021/ef990192n

Hower, JC, Senior, CL, Suuberg, EM, Hurt, RH, Wilcox, JL and **Olson, ES** 2010 Mercury capture by native fly ash carbons in coal-fired power plants. *Prog Energ Combust* **36**: 510–529. DOI: https://doi.org/10.1016/j.pecs.2009.12.003

Jaffé, R, Ding, Y, Niggemann, J, Vähätalo, AV, Stubbins, A, Spencer, RGM, Campbell, J and **Dittmar, T** 2013 Global charcoal mobilization from soils via dissolution and riverine transport to the oceans. *Science* **340**: 345–347. DOI: https://doi.org/10.1126/science.1231476

Johansson, L, Jalkanen, J-P and **Kukkonen, J** 2017 Global assessment of shipping emissions in 2015 on a high spatial and temporal resolution. *Atmos Environ* **167**: 403–415. DOI: https://doi.org/10.1016/j.atmosenv.2017.08.042

Jurado, E, Dachs, J, Duarte, CM and **Simóc, R** 2008 Atmospheric deposition of organic and black carbon to the global oceans. *Atmos Environ* **42**: 7931–7939. DOI: https://doi.org/10.1016/j.atmosenv.2008.07.029

Kanakidou, M, Duce, RA, Prospero, JM, Baker, AR, Benitez-Nelson, C, Dentener, FJ, Hunter, KA, Liss, PS, Mahowald, N, Okin, GS, Sarin, M, Tsigaridis, K, Uematsu, M, Zamora, LM and **Zhu, T** 2012 Atmospheric fluxes of organic N and P to the global ocean. *Global Biogeochem Cy* **26**, GB3026. DOI: https://doi.org/10.1029/2011GB004277

Koelmans, AA, Jonker, MTO, Cornelissen, G, Bucheli, TD, Van Noort, PCM and **Gustafsson, Ö** 2006 Black carbon: The reverse of its dark side. *Chemosphere* **63**: 365–377. DOI: https://doi.org/10.1016/j.chemosphere.2005.08.034

Koplitz, SN, Jacob, DJ, Sulprizio, MP, Myllyvirta, L and **Reid, C** 2017 Burden of disease from rising coal-fired power plant emissions in Southeast Asia. *Environ Sci Technol*. DOI: https://doi.org/10.1021/acs.est.6b03731

Külaots, I, Hsu, A, Hurt, RH and **Suuberg, EM** 2003 Adsorption of surfactants on unburned carbon in fly ash and development of a standardized foam index test. *Cem Concr Res* **33**: 2091–2099. DOI: https://doi.org/10.1016/S0008-8846(03)00232-1

Külaots, I, Hurt, RH and **Suuberg, EM** 2004 Size distribution of unburned carbon in coal fly ash and its implications. *Fuel* **83**(2): 223–230. DOI: https://doi.org/10.1016/S0016-2361(03)00255-2

Le, TPQ, Billen, G, Garnier, J, Théry, S, Fézard, C and **Chau, VM** 2005 Nutrient (N, P) budgets for the Red River basin (Vietnam and China). *Global Biogeochem Cy* **19**, GB2022. DOI: https://doi.org/10.1029/2004GB002405

Liang, B, Lehmann, J, Solomon, D, Kinyangi, J, Grossman, J, O'Neill, B, Skjemstad, JO, Thies, J, Luizao, FJ, Petersen, J and **Neves, EG** 2006 Black carbon increases cation exchange capacity in soils. *Soil Sci Soc Am J* **70**: 1719–1730. DOI: https://doi.org/10.2136/sssaj2005.0383

Lim, L, Wurl, O, Karuppiah, S and **Obbard, JP** 2007 Atmospheric wet deposition of PAHs to the sea-surface microlayer. *Mar Pollut Bull* **54**: 1212–1219. DOI: https://doi.org/10.1016/j.marpolbul.2007.03.023

Lin, J, Pan, D, Davis, SJ, Zhang, Q, He, K, Wang, C, Streets, DG, Wuebbles, DJ and **Guan, D** 2014 China's international trade and air pollution in the United States. *P Natl Acad Sci USA* **111**: 1736–1741. DOI: https://doi.org/10.1073/pnas.1312860111

Long, CM, Nascarella, MA and **Valberg, PA** 2013 Carbon black vs. black carbon and other airborne materials containing elemental carbon: Physical and chemical distinctions. *Environmental Pollution* **181**: 271–286. DOI: https://doi.org/10.1016/j.envpol.2013.06.009

Mannino, A and **Harvey, H** 2004 Black carbon in estuarine and coastal ocean dissolved organic matter. *Limnol Oceanogr* **49**: 735–740.

Manodori, L, Gambaro, A, Piazza, R, Ferrari, S, Stortini, AM, Moret, I and **Capodaglio, G** 2006 PCBs and PAHs in sea-surface microlayer and subsurface water samples of the Venice Lagoon (Italy). *Mar Pollut Bull* **52**(2): 184–192. DOI: https://doi.org/10.1016/j.marpolbul.2005.08.017

Mari, X, Lefèvre, J, Torréton, J-P, Bettarel, Y, Pringault, O, Rochelle-Newall, E, Marchesiello, P, Menkes, C, Rodier, M, Migon, C, Motegi, C, Weinbauer, MG and **Legendre, L** 2014 Effects of soot deposition on particle dynamics and microbial processes in marine surface waters. *Global Biogeochem Cy* **28**(7): 662–678. DOI: https://doi.org/10.1002/2014GB004878

Marques, JSJ, Dittmar, T, Niggemann, J, Almeida, MG, Gomez-Saez, GV and **Rezende, CE** 2017 Dissolved black carbon in the headwaters-to-ocean continuum of Paraíba do Sul River, Brazil. *Front Earth Sci* **5**: 11. DOI: https://doi.org/10.3389/feart.2017.00011

Marrero, J, Polla, G, Rebagliati, RJ, Plá, R, Gómez, D and **Smichowski, P** 2007 Characterization and determination of 28 elements in fly ashes collected in a thermal power plant in Argentina using different instrumental techniques. *Spectrochimica Acta Part B: Atomic Spectroscopy* **62**(2): 101–108. DOI: https://doi.org/10.1016/j.sab.2007.01.007

Masiello, CA and **Druffel, ERM** 1998 Black carbon in deep-sea sediments. *Science* **280**: 1911–1913. DOI: https://doi.org/10.1126/science.280.5371.1911

Mitra, S, Bianchi, TS, McKee, BA and **Sutula, M** 2002 Black carbon from the Mississippi River: Quantities, sources, and potential implications for the global carbon cycle. *Environ Sci Technol* **36**: 2296–2302. DOI: https://doi.org/10.1021/es015834b

Mitra, S, Zimmerman, AR, Hunsinger, GB and **Woerner, WR** 2014 Black carbon in coastal and large river systems. In *Biogeochemical Dynamics at Major River-Coastal Interfaces Linkages with Climate Change*, edited by Thomas S Bianchi, Mead A Allison, Wei-Jun Cai. Cambridge University Press, New York, NY, USA: 200–234.

Nguyen, TH, Brown, RA and **Ball, WP** 2004 An evaluation of thermal resistance as a measure of

black carbon content in diesel soot, wood char, and sediment. *Org Geochem* **35**: 217–234. DOI: https://doi.org/10.1016/j.orggeochem.2003.09.005

OECD 2016 The Economic Consequences of Outdoor Air Pollution, OECD Publishing, Paris. DOI: https://doi.org/10.1787/9789264257474-en

Ogren, JA and **Charlson, RJ** 1983 Elemental carbon in the atmosphere: cycle and lifetime. *Tellus* **35B**: 241–254.

Raimbault, P, Garcia, N and **Cerutti, F** 2008 Distribution of inorganic and organic nutrients in the South Pacific Ocean – evidence for long-term accumulation of organic matter in nitrogen-depleted waters. *Biogeosciences* **5**: 281–298.

Raimbault, P, Pouvesle, W, Diaz, F, Garcia, N and **Sempere, R** 1999 Wet-oxidation and automated colorimetry for simultaneous determination of organic carbon, nitrogen and phosphorus dissolved in seawater. *Mar Chem* **66**: 161–169. DOI: https://doi.org/10.1016/S0304-4203(99)00038-9

Ramanathan, V and **Carmichael, G** 2008 Global and regional climate changes due to black carbon. *Nat Geosci* **1**: 221–227. DOI: https://doi.org/10.1038/ngeo156

Ramanathan, V, Li, F, Ramana, MV, Praveen, PS, Kim, D, Corrigan, CE and **Nguyen, H** 2007 Atmospheric Brown Clouds: Hemispherical and regional variations in long range transport, absorption and radiative forcing. *J Geophys Res* **112**(D22): S21. DOI: https://doi.org/10.1029/2006JD008124

Rockne, KJ, Taghon, GL and **Kosson, DS** 2000 Pore structure of soot deposits from several combustion sources. *Chemosphere* **41**: 1125–1135. DOI: https://doi.org/10.1016/S0045-6535(00)00040-0

Seigneur, C, Aneck, H, Chia, G, Reinhard, M, Bloom, NS, Prestbo, E and **Saxena, P** 1998 Mercury adsorption to elemental carbon (soot) particles and atmospheric particulate matter. *Atmos Environ* **32**: 2649–2657. DOI: https://doi.org/10.1016/S1352-2310(97)00415-9

Smith, DM and **Chughtai, AR** 1995 The surface structure and reactivity of black carbon. *Colloids Surf A* **105**: 47–77. DOI: https://doi.org/10.1016/0927-7757(95)03337-1

Son, HD 2007 Study on establishing geographical basis for the rational use of Cua Luc Bay basin, Quang Ninh province. PhD Thesis, VNU-University of Science, Hanoi. 148 pages.

Stortini, AM, Martellini, T, Del Bubba, M, Lepri, L, Capodaglio, G and **Cincinelli, A** 2009 n-Alkanes, PAHs and surfactants in the sea surface microlayer and sea water samples of the Gerlache Inlet sea (Antarctica). *Microchem J* **92**(1): 37–43. DOI: https://doi.org/10.1016/j.microc.2008.11.005

Stubbins, A, Spencer, RGM, Mann, PJ, Holmes, RM, McClelland, JW, Niggemann, J and **Dittmar, T** 2015 Utilizing colored dissolved organic matter to derive dissolved black carbon export by arctic rivers. *Front Earth Sci* **3**: 63. DOI: https://doi.org/10.3389/feart.2015.00063

Styszko-Grochowiak, K, Gołas, J, Jankowski, H and **Koziński, S** 2004 Characterization of the coal fly ash for the purpose of improvement of industrial on-line measurement of unburned carbon content. *Fuel* **83**(13): 1847–1853. DOI: https://doi.org/10.1016/j.fuel.2004.03.005

Suman, DO, Kuhlbusch, TAJ and **Lim, B** 1997 Marine sediments: a reservoir for black carbon and their use as spatial and temporal records of combustion. In *Sediment Records of Biomass Burning and Global Change*. Clark JS, Cachier H, Goldammer JG, Stocks BJ (eds.), 271–293. Springer-Verlag, Berlin.

Ugurlu, A and **Salman, B** 1998 Phosphorus removal by fly ash. *Environ Int* **24**: 911–918. DOI: https://doi.org/10.1016/S0160-4120(98)00079-8

Wang, S and **Wu, H** 2006 Environmental-benign utilisation of fly ash as low-cost adsorbents. *J Hazard Mater* **136**: 482–501. DOI: https://doi.org/10.1016/j.jhazmat.2006.01.067

Wang, X, Xu, C, Druffel, ERM, Xue, Y and **Qi, Y** 2016 Two black carbon pools transported by the Changjiang and Huanghe Rivers in China. *Global Biogeochem Cy* **30**: 1778–1790. DOI: https://doi.org/10.1002/2016GB005509

Zerda, TW, Yuan, X, Moore, SM and **Leon y Leon, CA** 1999 Surface area, pore size distribution and microstructure of combustion engine deposits. *Carbon* **37**: 1999–2009. DOI: https://doi.org/10.1016/S0008-6223(99)00068-8

Ziolkowski, LA and **Druffel, ERM** 2010 Aged black carbon identified in marine dissolved organic carbon. *Geophys Res Lett* **37**(L16): 601. DOI: https://doi.org/10.1029/2010GL043963

How to cite this article: Mari, X, Chu Van, T, Guinot, B, Brune, J, Lefebvre, J-P, Raimbault, P, Dittmar, T and Niggemann, J 2017 Seasonal dynamics of atmospheric and river inputs of black carbon, and impacts on biogeochemical cycles in Halong Bay, Vietnam. *Elem Sci Anth,* 5: 75. DOI: https://doi.org/10.1525/elementa.255

Domain Editor-in-Chief: Jody W. Deming, University of Washington, US

Associate Editor: Laurenz Thomsen, Jacobs University Bremen, DE

Knowledge Domain: Ocean Science

Part of an *Elementa* Special Feature: The Sea Surface Microlayer – Linking the Ocean and Atmosphere

Submitted: 14 February 2017 **Accepted:** 17 October 2017 **Published:** 06 December 2017

ELEMENTA Science of the Anthropocene

Elem Sci Anth is a peer-reviewed open access journal published by University of California Press.

OPEN ACCESS